# Biogeochemistry of the flora of Weda Bay, Halmahera Island (Indonesia) focusing on nickel hyperaccumulation

Severine Lopez, Peter D. Erskine, Yannick Cazes, Jean-Louis Morel, Gavin Lee, Edi Permana, Guillaume Echevarria, Antony van Der Ent

# Biogeochemistry of the flora of Weda Bay, Halmahera Island (Indonesia) focusing on nickel hyperaccumulation

Séverine Lopez[1], Emile Benizri[1], Peter D. Erskine[2], Yannick Cazes[1], Jean Louis Morel[1], Gavin Lee[3], Edi Permana[3], Guillaume Echevarria[1], Antony van der Ent[1, 2,*]

[1]Université de Lorraine, INRA, Laboratoire Sols et Environnement, France.

[2]Centre for Mined Land Rehabilitation, Sustainable Minerals Institute, The University of Queensland, Australia.

[3]PT Weda Bay Nickel, Indonesia.

[*]Corresponding author, Centre for Mined Land Rehabilitation, Sustainable Minerals Institute, The University of Queensland, St Lucia 4072 QLD, Australia, e-mail: a.vanderent@uq.edu.au

**ABSTRACT**

Indonesia has one of the largest surface expressions of ultramafic rocks on Earth and in parallel hosts one of the most species-rich floras. Despite the extensive knowledge of the botanical diversity and the chemistry of these substrates, until recently the records for nickel hyperaccumulators in the region have been scant. Identification of native local hyperaccumulator species is the critical initial step for phytomining as these species match ambient bioclimatic, geochemical and physiological conditions. Prior to this research just 11 nickel hyperaccumulators were known from Indonesia. This field-based investigation at Weda Bay revealed the existence of 13 nickel and two cobalt hyperaccumulators. Phylogenetic affinity for nickel hyperaccumulation is diverse and spans several orders but was most frequent in the Malpighiales as in other ultramafic regions of Southeast Asia. In contrast to global patterns, hyperaccumulation was infrequent in the Phyllanthaceae.

**Keywords**: *biogeochemical cycling*, *hyperaccumulator, trace element, ultramafic, nickel*

## 1. INTRODUCTION

Ultramafic bedrock is part of the upper mantle (peridotite) obducted in continental margins (Searle and Stevens, 1984). Such outcrops are widespread but relatively rare, covering > 3% of the surface of the earth (Guillot and Hattori, 2013). Southeast Asia has some of the largest tropical outcrops in the world with Borneo and Sulawesi together totalling over 23 000 $km^2$ (van der Ent et al., 2013b; Galey et al., 2017). Ultramafic soils have high concentrations of iron (Fe) and magnesium (Mg), are enriched in nickel (Ni), chromium (Cr) and cobalt (Co), and are phosphorus (P) and potassium (K) deficient (Proctor, 2003). The atypical soil chemistry has caused the occurrence of distinct vegetation types characterized by relatively low stature and high levels of endemicity (Brooks, 1987; Proctor, 2003; Rajakaruna and Baker, 2004). Hyperaccumulators are unusual plants that accumulate trace elements to exceptional concentrations in their living tissues at orders of magnitude greater concentrations than 'normal' plants (Baker and Brooks, 1989; van der Ent et al., 2013a). Some of these plants can reach up to 7.6% Ni in leaves (Mesjasz-Przybyłowicz et al., 2004) and up to 16.9 dry Wt% the phloem sap (van der Ent and Mulligan, 2015). Hyperaccumulator plants can achieve such extraordinary levels of accumulation due to enhanced uptake and translocation mechanisms from the roots to the shoots (Baker, 1981; 1987). Trace element hyperaccumulation is defined as foliar concentrations in excess >300 mg $kg^{-1}$ of Co, >1000 mg $kg^{-1}$ of Ni, >10 000 mg $kg^{-1}$ of Mn when growing in natural habitats (Baker and Brooks, 1989; Reeves, 2003; van der Ent et al., 2013a).

On a global scale, Ni hyperaccumulation is the most prevalent, with approximately 520 species reported to date, of which just ~50 *hypernickelophores* (*e.g.* hyperaccumulator species with >1 Wt% shoot dry weight) are known globally (Reeves, 2003; Reeves et al., 2018a). Hyperaccumulation is a rare phenomenon occurring in 0.2% of total angiosperms (Baker, 1981; Baker and Brooks, 1989) and up to two percent of the ultramafic flora (van der Ent *et al*., 2015b). The greatest number of Ni hyperaccumulators has been reported from Cuba (130) and New Caledonia (65) (Reeves et al., 2018b; Jaffré et al., 2013), and recently Sabah (Borneo Island) also emerged as a hotspot for Ni hyperaccumulators with the recording of 25 species (van der Ent et al., 2015b; 2016b). Nickel hyperaccumulators can be categorised in either obligate or facultative species, the former restricted to ultramafic soils and displaying hyperaccumulation, the latter with populations on non-ultramafic and ultramafic soils but only displaying hyperaccumulation on the ultramafic soils (Pollard et al., 2014). The ecology and natural selection of hyperaccumulator plants is an active field of inquiry, focussing on anti-herbivore defences, allelopathy and biotic interactions (Martens and Boyd, 1994; Boyd and Martens, 1998; Jaffré et al., 2018). Nickel hyperaccumulator

plants have the potential to be used in phytomining, an environmentally sustainable technology to produce Ni (Chaney, 1983; Chaney et al., 2007; van der Ent et al., 2015a). In a phytomining operation, hyperaccumulator plants are grown on ultramafic soils, followed by harvesting and incineration of the biomass to generate a commercial high-grade Ni bio-ore (Chaney et al., 2007; Barbaroux et al., 2011; Van der Ent et al., 2015a).

Nickel hyperaccumulators have been recorded from at least 40 different plant families (Reeves, 2006), but are most prevalent in the order Brassicales (Brassicaceae, genera *Odontarrhena* [synonym *Alyssum*], *Arabidopsis, Bornmuellera* [synonym *Leptoplax*], *Noccaea*) in temperate regions and in the Asterales (*Berkheya, Pentacalia, Senecio*), the Buxales (Buxaceae; Buxus) and the supraordinal COM clade (Celastrales, Oxalidales, Malpighiales, mainly Euphorbiaceae, Phyllanthaceae, Salicaceae and Violaceae families) in tropical regions. In Southeast Asia, Ni hyperaccumulator plants are predominantly from the Malpighiales order, and particularly the Phyllanthaceae family (van der Ent et al., 2015b; Galey et al., 2017). The Malpighiales is one the most diverse groups of flowering plants, comprising about 8% of all eudicots and 6% of all angiosperms (Davis et al., 2005; Korotkova et al., 2009), and hyperaccumulators are mainly represented in the Phyllanthaceae in the genera, *Actephila, Antidesma, Breynia, Cleistanthus, Glochidion* and *Phyllanthus* (van der Ent et al., 2015b). The latter is cosmopolitan and the most speciose genus with over 800 species globally, with major centres of diversity in New Caledonia (113 species) and Cuba where Ni hyperaccumulators are numerous (Reeves et al., 1996; Reeves et al., 1999). Limited systematic screening across phylogenetic lineages means that at present there is no comprehensive understanding of the phenomenon, although such efforts are currently underway using XRF devices (Gei et al., 2018) followed by detailed investigations of their ecophysiology using advances techniques such as synchrotron-based X-ray Fluorescence Microscopy (van der Ent et al., 2017a,b). Hyperaccumulator discoveries continue to be made in Southeast Asia, such as *Antidesma montis-silam* from Sabah (Nkrumah et al., 2018), and even new species that are hyperaccumulators, are described, such as *Actephila alanbakeri* (van der Ent et al., 2016b) and *Phyllanthus rufuschaneyi* (Bouman et al., 2018) both from Sabah. The search for hyperaccumulators has been limited to date in Indonesia. Analysis of herbarium specimens originating from Indonesia led to the discovery of the following Ni hyperaccumulators: *Rinorea bengalensis, R. javanica* (Violaceae), *Trichospermum kjelbergii* (Tiliaceae), *Planchonella oxyhedra* (Sapotaceae), *Myristica laurifolia* var. *bifurcata* (Myristicaceae), *Brackenridgea palustris* subsp. *kjellbergii* (Ochnaceae), *Psychotria* sp. (Rubiaceae), *Phyllanthus insulae-japen* and *Glochidion* aff. *acustylum* (Phyllanthaceae) (Wither and Brooks, 1977; Reeves, 2003). More recently, fieldwork in

Sulawesi recorded *Sarcotheca celebica* (Oxalidaceae) and *Knema matanensis* (Myristicaceae) as Ni hyperaccumulators (Tjoa, pers. comm.; van der Ent et al., 2013b).

Ultramafic rock is serpentinised to varying degrees, and serpentinite is used to describe rocks containing >50% serpentine group minerals in which the original mineralogy has been changed. Ultramafic rock generally itself only contains 0.16–0.4% Ni (Butt and Cluzel, 2013) but this increases significantly during surface weathering in humid tropical climates (Echevarria, 2018) becomes atarget. Where they occur, ultramafic ecosystems are renowned for high levels of endemism, especially in Southeast Asia (Galey et al., 2017). At the same time, ultramafic outcrops holding Ni-rich laterites are Ni mining targets in the Indonesian region. That brings the minerals industry capitalizing on Ni resources in direct conflict with biodiversity. The Weda Bay project in Halmahera has a contract area of 54 874 ha with an estimated resource of 5.1 Mt of Ni and targeted annual capacity of 65 kt $yr^{-1}$ in Ni. This study aims to provide baseline data on the biogeochemistry of the ultramafic soils of Weda Bay Nickel (WBN) mine lease on Halmahera Island in Indonesia. Specifically, the objectives of this research were to screen for the possible occurrence of hyperaccumulator plants, to provide information on the foliar chemistry, and to provide an indicative assessment of the potential for phytomining at Weda Bay Nickel.

## 2. MATERIALS AND METHODS

### 2.1 Study area and sample collection

During the fieldwork, a total of 21 non-permanent plots (see Figure 1 for locations and Table 1 for site properties) were made in which 817 herbarium vouchers and associated foliar samples, in addition to soil samples (totalling 85 samples), were collected for laboratory analysis. Plants were screened in the field (>1000 specimens) for Ni hyperaccumulation using dimethylglyoxime impregnated test paper, and after positive reaction detailed samples were collected for these hyperaccumulator plants. This included samples of the rhizosphere soil, root, wood, branches and leaves. In total 13 Ni hyperaccumulators species, 2 Co, 1 Mn and 10 Al hyperaccumulators were discovered, and associated plant tissue samples totalling 316 samples with 46 matching rhizosphere soil samples collected. The current work does not discuss the hyperaccumulator species from Weda Bay, and we refer to Lopez *et al.* (2019a, b) for more information about the individual hyperaccumulator species and the rhizosphere chemistry. Concentrations of Ni and other elements were determined in the field with a handheld X-Ray Fluorescence (XRF) instrument. Fresh plant leaves were put in paper bags to prevent decomposition before transport to the field station. Leaves were dried at 70°C for five days in a dehydrating oven. Soil samples were collected from the centre of 15 sites. After an elimination of the surface organic plant debris, organo-mineral horizons were

sampled at a depth between 0–5 cm below litter and mineral horizons were sampled at a depth of 10–25 cm depending on the soil type in order to avoid the organo-mineral horizon. In all cases, except for Leptosols, it corresponded to either the Cambic horizon or the Ferralic horizon. The 30 soil samples were air-dried and then sieved to 2 mm before storage and analyses.

**2.2 Chemical analyses of plant tissue samples**

Foliar samples were crushed and ground, and a 500-mg subsample was digested in 3 mL concentrated nitric acid (65%) and 1 mL hydrogen peroxide (30%) for 2 hours at 95°C. The digest was diluted to 40 mL with ultra-pure water before analysis with ICP-AES (Liberty II, Varian). Elements included in the analysis were Ni, Co, Cr, Cu, Zn, Mn, Fe, Mg, Ca, Na, K, S and P. The potential for foliar contamination with soil particulates is a major risk for accurate analysis of foliar elemental composition. This risk is highest in samples of ground-herbs, and lesser so for trees, but it cannot be entirely avoided. Concomitantly high foliar concentrations of Fe (>2500 μg $g^{-1}$) and Cr (>50 μg $g^{-1}$) are an indication for soil contamination as these elements are major constituents of ultramafic soils.

**2.3 Chemical analyses of soil samples**

Soil samples (500 mg subsample) were acid-digested using freshly prepared Aqua Regia (6 mL 37% hydrochloric acid and 2 mL 70% nitric acid per sample) for a 2-hour program and diluted with ultra-pure water to 50 mL before ICP-AES analysis of pseudo-total elements for Ni, Co, Cu, Zn, Mn, Fe, Mg, Ca, Na, K, S and P. Soil pH was measured in a 1:5 soil : water mixture. Exchangeable Ni, Co, Cr and Mn were extracted in 0.0166 M [$Co(NH_3)_6^{3+}$, $3Cl^-$] at a soil : solution ratio of 1:20 (2.5 g : 50 mL) and 1 hour shaking time according to international ISO standard 23470 (ISO 23470:2007). Extractable Ni, Cr and Mn in soil samples were obtained from a DTPA–TEA solution (0.005 M diethylene triamine pentaacetic acid, 0.01 M calcium chloride, 0.1 M triethanolamine, pH 7.4) according to Lindsay and Norvell (1978) and concentrations in solutions were measured with ICP-AES (Liberty II, Varian). Total C and N and organic C were quantified by combustion at 900 °C with a CHNS analyser (vario MICRO cube, Elementar Analysensysteme GmbH). Soil samples were weighed using a four-decimal balance and weights recorded for correction of the precise weights in the mass balance calculations. Samples were agitated for method-specific times using an end-over-end shaker at 60 rpm and subsequently centrifuged (10 minutes at 4000 rpm). All soil samples were analysed with ICP-AES (Liberty II, Varian) for Ni, Co, Cu, Zn, Mn, Fe, Mg, Ca, Na, K, S and P. The ICP-AES instrument was calibrated using a multi-element standard prepared in each extraction solution and internal standards were used to ensure of the reliability of ICP-AES analysis.

170

171 **2.4 Mineralogical analyses of soil samples by X-Ray Diffraction (XRD)**

172 The dry samples from the soils from the 15 sites were ground and sieved to 80 µm for mineralogical
173 analysis by XRD. X-Ray diffraction (XRD) analysis was performed on the selected samples using a
174 D8 Bruker diffractometer with Co $K_{\alpha}^{1}$ radiation (lambda = 1.7902 Å). The diffractometer is
175 equipped with a (θ, 2θ) goniometer and a position sensitive detector (PSD). X-ray diffractograms
176 were collected on powder samples at room atmosphere and temperature, within the 2theta range [3,
177 65°], with 0.035° step and 2s collecting time.

178

179 **2.5 Statistical analysis**

180 The ranges and means of the foliar and soil concentrations were calculated. Correlation coefficients
181 between the soil and plant chemistry data were also calculated. These analyses were undertaken
182 using the software packages STATISTICA Version 9.0 (StatSoft), Excel for Mac version 2011
183 (Microsoft) and R software (version 3.3.1).

184

185 **3. RESULTS**

186

187 **3.1 Field survey and hyperaccumulator plant species**

188 The Weda Bay area consists largely of a 'mosaic' of secondary vegetation with patches of more
189 intact forest, and vegetation, which have experienced recurrent fires, particularly near the coast
190 (Figure 2). The highest plant diversity was encountered at the Casuarina site (secondary lowland
191 forest on serpentinite) and at Jira (secondary lowland forest on a laterite plateau). Prior to this field
192 survey no Ni hyperaccumulator plants were known from Halmahera Island, and just five
193 hyperaccumulators were known from Indonesia (van der Ent et al. 2013b). The fieldwork yielded
194 13 Ni hyperaccumulator plants from the locations survey (including Bukit Limber, Sake South,
195 Sake, Sake West, Uni-Uni, Casuarina) (Table 1). The hyperaccumulator plants originated from a
196 range of different families, and several records included families Anacardiaceae, Apocynaceae,
197 Aristolochiaceae, Moraceae, Piperaceae and Rosaceae that were not previously known to contain Ni
198 hyperaccumulating taxa. Several Ni hyperaccumulator species are locally common and occur
199 widespread at Weda Bay, namely *R.* aff. *bengalensis, Planchonella roxburghiana, F. trachypison*
200 and *T. morotaiense*. Burnt vegetation in the coastal areas was relatively species poor but hosted all
201 13 Ni discovered hyperaccumulator species including at Sake South and Casuarina. *Rinorea* aff.
202 *bengalensis* (Violaceae) is clearly closely-related to the widespread *R. bengalensis* (Sri Lanka to
203 Northeast Australia), but has morphological differences warranting typification as a distinct taxon
204 (J. DeMuria pers. comm.). It occurs as an under-storey shrub or small tree (up to 10 m tall and a

bole of 20 cm diameter) in dense secondary vegetation and short-statured forest on Cambisols. *Ficus trachypison* is the sole Ni hyperaccumulating taxon from the genus *Ficus* and the family Moraceae known globally. It is exceedingly common as a pioneer in degraded (burnt) scrub in the coastal areas, such as at Sake River, and Location 2A–C on Hypereutric Cambisols. One of the most interesting species, because it is a facultative Ni hyperaccumulator, is *Trichospermum morotaiense* (Tiliaceae). This medium to large tree (up to 20 m tall and a bole of 40 cm diameter) occurs mainly in riparian habitats on ultramafic soils (where it hyperaccumulates Ni) and on limestone (where it does not hyperaccumulate Ni). The genus *Trichospermum* has 36 species occurring predominantly in Malesia but distributed from Malaysia to the Solomon Islands and Fiji and Samoa, with most species in New Guinea (Kostermans, 1972). *Trichospermum kjelbergii* from Sulawesi was one of the first Ni hyperaccumulators to be discovered in Indonesia (Wither and Brooks, 1977). *Planchonella roxburghiana* (Sapotaceae) is a medium-sized tree (up to 15 m tall and with a bole of 25 cm diameter) that occurs in medium tall lowland forest (<20 m) on Hypereutric Rhodic Cambisols. This species is slow-growing, judging by its hard timber, and closely related to *Planchonella oxyhedra* recorded as a Ni hyperaccumulator from Central Sulawesi (Wither and Brooks, 1977). No Ni hyperaccumulators were found at higher elevations (>500 m asl), such as at Bukit Limber 900–1000 m asl, which has lower montane forest. This may be explained by the low extractability of Ni and acidic pH in the Rhodic Plinthic Ferralsols of this site. Similarly, Ni hyperaccumulators were absent from Uni-Uni, which has Geric Plinthic Rhodic Ferralsols, with the exception of *Glochidion moluccanum* (Phyllanthaceae). The latter is a pioneer shrub (no more than 3 m tall) that is common in the graminoid scrub at Uni-Uni that has been repeatedly burnt. We refer to Lopez *et al.* (2019a, b) for more detailed information about the individual hyperaccumulator species.

### 3.2 Soil mineralogy and soil types

The diffractograms of the soils, both organo-mineral (0–5 cm layer) and mineral (10–25 cm layer) horizons sampled on 15 sites (30 soil samples) were acquired to indicate the weathering status of each pedon as well as the nature of the bedrock (*e.g.* degree of serpentinisation of the peridotite). Diffractograms from organo-mineral horizons were usually less easily interpreted because of the high background noise created by the high organic matter content. Therefore, the mineralogy of mineral horizons was used to describe soils (Table 2) except for the soil on Limestone for which the best diffractogram was from the organo-mineral horizon (lack of clay minerals in the mineral horizon). Primary minerals derived from ultramafic soils were either from non-serpentinised peridotite (*i.e.* diopside, enstatite, tremolite, fayalite) or from serpentinite (*i.e.* talc, serpentine, magnetite). Secondary minerals were mainly clays (smectite group clays, probably montmorillonite

in all the cases) and iron oxides (*i.e.* goethite and hematite). None of the soils had pyroxenes or olivines as major mineral constituents, although some soils contained traces of these minerals (Blue Hill, Casuarina Plot 1, 2B and Woi Mioseng). One soil had tremolite as its major mineral constituent (Casuarina Plot 2). Serpentine (mostly chrysotile and in one case clino-chrysotile: Bukit Limber Plot 1) is the dominating mineral phase in the soils Blue Hill (co-dominating with serpentine), Uni-Uni Plot 1 and Woi Mioseng). Secondary smectites dominate the mineralogy of Blue Hill, and Location 2A, 2B and 2C. The mineralogy of the rest of ultramafic soils was dominated by secondary goethite. Quartz can be considered as a secondary mineral in most of the soils where it is present. Calcite was the only primary mineral detected for the Leptosol of Doromesmesan and only some clays and traces of quartz could be detected in the organo-mineral horizon. The mineral horizon was pure calcite on this soil. The variety of mineralogical profiles (most representative profiles) is shown in Figure 5.

The soils, according to their morphology (field observations), chemistry and mineralogy could be classified as the following types (Table 1): Rendzic Leptosol on Limestone; Hypereutric Leptosols (Hypermagnesic) and Hypereutric Leptic Cambisols (Hypermagnesic) on Serpentinite; Ferralic Rhodic Cambisols on poorly serpentinised Peridotite and Geric Plinthic Ferralsols on non-serpentinised peridotites (including dunite). This variety of soils created a wide array of edaphic conditions from low pH soils with no exchangeable cations, to neutral and high pH soils with a CEC saturated with Mg. Also, the soils varied deeply from very shallow Leptosols (Blue Hill and Doromesmesan) to very deep laterites (Bukit Limber Plots 1 & 2 and Uni-Uni Plot 1), thus providing a wide array of physical properties for ecosystem processes (shallow *vs.* deep rooting).

### 3.3 Soil chemical characteristics in the surveyed area

Thirty soil samples were derived from (serpentinised) ultramafic bedrock and one was a Rendzic Leptosol on Limestone (Doromesmesan). Chemical properties of mineral (10–25 cm layer) and organo-mineral (0–5 cm layer) soil samples from each site are presented in Tables 3 to 8. These mineral (Table 3) and organo-mineral (Table 4) horizons showed amounts of total Fe ranging from 1.5 to 39.8%, total Mg from 0.8 to 13.3%. They were all characterized by low concentrations of Ca, P (less than 0.04%) and K (less than 0.03%) excepted for the site Location 2C with 0.05 and 0.08 for the mineral and organo-mineral horizons, respectively. These values and the high values of Ni, which ranged from 87 to 13,587 mg $kg^{-1}$, confirmed the ultramafic origin of these different soil samples.

The DTPA-extractable elements (such as Ca, Mg, and K) of the organo-mineral horizons (Table 6) had the highest values in comparison to mineral horizons (Table 5), except for Fe and Mg. DTPA-extractable Ni concentrations reached 772 mg $kg^{-1}$ in Sake South soil.

The pH ranged from 4.07 to 8.16 in the mineral horizons (Table 7) and from 4.65 to 8.07 in the organo-mineral horizons (Table 8). Some Ferralsols or soils with Ferralic properties were present in the collection (*e.g.* soils from Bukit Limber plot 2, Sake West, Uni-Uni plot 1) and their pH ranged from 4.07 to 5.31 for mineral horizons and from 4.65 to 6.59 for organo-mineral horizons, in the lower of the total range. Also, these soils had very low Cation Exchange Capacity (CEC), with values ranging from 2.04 to 5.05 and from 4.32 to 8.66 $cmol^{+}\ kg^{-1}$, respectively for mineral and organo-mineral horizons, compared to the whole collection (from 2.04 to 53.7 and from 4.32 to 64.3 $cmol^{+}\ kg^{-1}$, respectively for mineral and organo-mineral horizons). These soils were characterized by low exchangeable Mg values compared to the whole range of soils: their Mg-CEC ranged from 0.07 to 1.2 and from 0.38 to 4.1 $cmol^{+}\ kg^{-1}$, respectively for mineral and organo-mineral soils. The other soils were (Hyper)Eutric Cambisols (Hyper)Magnesic and were also widely present in the area. Their pH was higher in general (ranging from 6.06 to 8.16 and from 6.01 to 7.41, respectively for mineral and organo-mineral horizons) and so was their CEC (presence of high-charge clays and higher organic matter contents) which ranged from 4.40 to 53.7 and from 7.49 to 64.3 $cmol^{+}\ kg^{-1}$, respectively for mineral and organo-mineral soils. Most of the CEC values for these Cambisols were above 20.0 $cmol^{+}\ kg^{-1}$. The maximum reported values for Mg-CEC were reported also for these soils and reached 50 and 40 $cmol^{+}\ kg^{-1}$, respectively for mineral and organo-mineral horizons. The Rendzic Leptosol sampled from the site Doro Mesmesan Limestone Plot 1 showed particular values as it was not ultramafic with alkaline pH, high amount of total Ca and P but low Fe and Mg concentration (Table 3 and 4), inducing a Ca/Mg ratio of 36–46. The CEC was also greater in comparison with the other soils. The CEC in all soils was mostly influenced by the organic matter content (Tables 7 and 8) and the amount of smectite-type clays in the mineral phases (Table 2).

Soil weathering tends to favour Ca retention on the CEC and Mg leaching (Echevarria, 2018) and exchangeable Ca was greater in organo-mineral horizons than in mineral horizons for all soils, whereas it was the exact opposite for Mg. Therefore, most of the Ferralsols were not Magnesic, whereas all Cambisols were Magnesic or Hypermagnesic.

The mean total Ni concentrations were 4.16 mg $g^{-1}$ (0.3–14.0 mg $g^{-1}$) and 3.77 mg $g^{-1}$ (0.1–12.0 mg $g^{-1}$), respectively for mineral and organo-mineral soils. Exchangeable Ni (Ni-CEC) was

usually quite low compared to Mg or to Ca (being the major exchangeable cations) and ranged, when detected, from 0.01 to 0.29 $cmol^+ kg^{-1}$ in mineral horizons and from 0.01 to 0.39 $cmol^+ kg^{-1}$ in organo-mineral horizons. There is no clear contrast between the two horizons: in some soils it was higher in the OM-rich horizons (mostly Ferralsols), whereas it was the opposite in some others (mostly Cambisols). In the Ferralic Rhodic Eutric Cambisol (Magnesic) from Sake South, there was an unusually high concentration of Ni-CEC in both horizons (1.2–1.4 $cmol^+ kg^{-1}$). In this soil, Ni saturated 6.0 to 8.2 % of the total CEC. The DTPA-extractable Ni ($Ni_{DTPA}$) was moderate to high with 4.0 to 704 and 0.1 to 773 $\mu g\, g^{-1}$, respectively for mineral and organo-mineral soils. Ferralsols had $Ni_{DTPA}$ values ranging from 4.0 to 17 $\mu g\, g^{-1}$ (with lower values in mineral soils), whereas Cambisols had higher values ranging from 14 to 773 $\mu g\, g^{-1}$. Again, as for Ni-CEC, the greatest values that were above 700 $\mu g\, g^{-1}$ also corresponded to the soil from Sake South, which is somewhat an intergrade soil between Cambisols and Ferralsols.

### 3.4 Plant foliar chemistry

The 724 leaves from non-hyperaccumulator plants and the 93 leaves from Ni-hyperaccumulator plants were sampled in 21 different ultramafic sites. Based on concentrations measured in soil and foliar parts, the accumulation potential of different elements (Na, Mg, Al, P, S, K, Ca, Mn, Fe, Ni and Zn) was presented for non-hyperaccumulator (Figure 6A) and Ni-hyperaccumulator (Figure 6B) plants. Based on a nonparametric Wilcoxon-Mann-Whitney statistical test, there were significant differences between the ability of non-hyperaccumulator and hyperaccumulator plants to extract all the elements considered.

For the three elements Ca, K and P, plants can be considered as accumulators, with a concentration in their leaves greater than the concentration in soils. This observation was the same whatever the plants; hyperaccumulators or non-hyperaccumulators. Indeed, the mean foliar concentrations were around 15 g $kg^{-1}$ for Ca, 7.9 g $kg^{-1}$ for K and 530 mg $kg^{-1}$ for P (Supplementary information, Tables 1 and 3). These very low foliar P concentrations were typical for tropical rain forests plants, as observed by many authors (Vitousek and Sanford, 1983; Kitayama et al., 2000; Vitousek et al., 2010). Conversely, hyperaccumulator and non-hyperaccumulator plants here should be considered as excluders for Mg and Mn; these elements showed lower concentrations in plant parts in comparison with those measured in soils whatever the plant considered (Supplementary information, Table 1 to 4). In total, 10 different Al hyperaccumulator plants were recorded (Table 10). There were 5 other Al hyperaccumulator records exceeding the nominal threshold (>1000 mg $kg^{-1}$), but these plants remain unidentified. The identified Al hyperaccumulators were phylogenetically diverse (originating from 7 different families), although three species of

*Symplocos* (Symplocaceae) were prominent at higher altitudes in cloud forest on Bukit Limber. The highest concentration was found in *Symplocos maliliensis* with 46 300 mg $kg^{-1}$ foliar Al. *Symplocos* is a well-known genus of Al hyperaccumulators from Southeast Asia (Chenery, 1949; Schmitt et al., 2016).

There were clear differences concerning foliar concentrations of the elements Al, Fe, Na, S, Zn and Ni (Supplementary information, Tables 1 to 4), between the two plant types (*i.e.* Ni hyperaccumulator and non-hyperaccumulator plants). For example, Al leaf concentrations for Ni hyperaccumulator and non-hyperaccumulator plants were around 20 and 210 mg $kg^{-1}$, respectively, with a concentration 10.5 times greater for non-hyperaccumulators. This is due to the fact that the higher concentration for Ni hyperaccumulators was around 260 mg $kg^{-1}$ while it was around 35 000 mg $kg^{-1}$ for other plants, including Al hyperaccumulators obviously. All Al hyperaccumulators (that did not accumulate Ni at all) were reported from sites with Ferralsols (Uni-Uni plot 2, Bukit Limber plots 1 & 2 and Jira plot 1). Conversely, the foliar concentrations for Na and S were higher for hyperaccumulator plants in comparison with non-hyperaccumulators: the concentrations were around 1700 and 1300 mg $kg^{-1}$ for Na and 2300 and 1900 mg $kg^{-1}$ for S, respectively for hyperaccumulator and non-hyperaccumulator plants, revealing a higher capability of the hyperaccumulator plants to extract these elements (Na and S). The same trend was observed for Zn. Indeed, we found a three-fold higher Zn concentration in Ni hyperaccumulators with approximately 70 mg $kg^{-1}$, while the concentration in other plants was around 25 mg $kg^{-1}$.

The most important difference was found in the foliar concentrations of Ni hyperaccumulators *vs.* non-hyperaccumulators. The mean Ni concentration was ~5500 mg $kg^{-1}$ for the hyperaccumulators, while it was ~230 mg $kg^{-1}$ for the non-hyperaccumulators. These important differences between non-hyperaccumulator and hyperaccumulator samples were underlined by the distribution, based on the Ni concentrations in leaves, of the number of non-hyperaccumulator samples and hyperaccumulator samples (Figures 6 and 8). Moreover, a clear difference between these two types of plants was highlighted, particularly for most of the measured elements in the leaves (Al, Ca, Fe, K, Na, Co, S and Zn). Indeed, the distribution of leaves samples concerning the different elements, such as Fe, Mn, Na and Zn, confirmed the trend that the Ni hyperaccumulator plants can extract higher amounts of these elements, in comparison with the non-hyperaccumulators. The same trend was observed for Co with concentrations around 35 and 2.5 mg $kg^{-1}$, respectively for hyperaccumulator and non-hyperaccumulator plants, revealing a concentration 14 times greater for hyperaccumulators.

As shown in Figure 7, based on the DTPA-extractable metal concentrations measured in soils and Ni concentrations in plant parts, Ni hyperaccumulator plants have a higher ability to extract other strategic metals such as Mn, Co and Zn compared to non-hyperaccumulator plants. The difference is not clear for Mn, with a ratio of DTPA-extractable metal present in the soil and leaf concentration of 6.9 and 5.6 for hyperaccumulators and non-hyperaccumulators, respectively. Zn non-hyperaccumulator plants were able to concentrate in their foliar parts 9.5-times the DTPA-extractable Zn present in the soil, whereas the hyperaccumulator plants showed a ratio of 25.5, *i.e.* 2.7-times more in comparison with non-hyperaccumulator plants. For Co, the non-hyperaccumulator plants showed a foliar concentration equivalent to that of the DTPA-extractable Co concentrations found in the soil, but the hyperaccumulator plants were able to concentrate this metal about 14-times more in comparison with non-hyperaccumulator plants. Based on the comparison of foliar metal concentrations and DTPA metal concentrations present in the soil, the best comportment appeared for Ni. Indeed, the non-hyperaccumulator plants concentrated this element up to 1.5-times, while the concentrations in the areal parts of hyperaccumulator plants were 27.5-times higher than the DTPA concentrations in soils, that to say 19-times more than the non-hyperaccumulator plants.

### 3.5 Parasitic mistletoe on the Ni (hyper)accumulator *Ficus trachypison*

The mistletoe *Amyema cuernosensis* (Loranthaceae) was recorded parasitizing on the Ni (hyper)accumulator *F. trachypison* near the Casuarina site (Figure 9, Table 11). It accumulated up to 341 mg $kg^{-1}$ Ni which can only be acquired from the host since it is an obligate parasite with no root system. The Ni concentrations in the stem and in the leaves of the host plant, *i.e. F. trachypison*, were 3.0 and 217 mg $kg^{-1}$ Ni respectively.

## 4. DISCUSSION

The specific genesis and geochemistry of ultramafic soils is crucial to understand the occurrence of hyperaccumulation and Ni hyperaccumulators (Echevarria, 2018; van der Ent et al., 2016a). It was not always possible during this survey to access the bedrock at each location in order to describe it, but when it was and described, it was clear that the soil characteristics (soil genesis and functioning) was highly influenced by the degree of serpentinisation of the peridotite (van der Ent et al., 2018a). The areas covered by strongly serpentinised peridotite or serpentinite always had Cambisols with neutral pH and Mg as the main exchangeable cation in the CEC. These soils had very high level of available Ni. These Hypereutric Cambisols (Hypermagnesic) are derived from strongly serpentinised ultramafic bedrock in which the most important Ni-bearing phases are likely hydrous

and crystalline ferrous oxides and smectite minerals in which Ni is either sorbed or included in the crystal lattice (Echevarria, 2018). Like other ultramafic soil covers in tropical areas (Proctor, 2003; Echevarria, 2018), the mineralogy of Cambisols on serpentinite at Weda Bay was often dominated by smectites in the weathered horizon ($B_W$). The Ferralsols presented several degrees of evolution, probably because of the hilly landscape that induces soil erosion and rejuvenation (Echevarria, 2018). The most developed soil profiles were found at high altitude on the plateau at Bukit Limber (ca. 1000 m asl.) and at Uni-Uni at a lower altitude (ca. 260 m asl.). The former had the deepest profile development with a 30-m lateritic development in places (as was visible from a mining test pit). The ultramafic region at Weda Bay has therefore a varied gradient of tropical ultramafic pedogenesis.

One surprising finding was that the highest DTPA-extractable Ni concentration ever recorded in an ultramafic soil (Echevarria, 2018; van der Ent et al., 2018a) was from a soil that was not a typical Hypereutric Cambisol (Hypermagnesic). It was a Ferralic Cambisol (Magnesic), halfway between a typical ultramafic Hypermagnesic Cambisol and a Geric Plinthic Rhodic Ferralsol. This soil was very rich in total Ni (1.4 %) and had a pH of 5.92. The soil hosted strong Ni hyperaccumulators (some displaying Ni concentrations in their leaves above 2.2 %) although a study in Sabah (Borneo Island) showed that Ni hyperaccumulators are absent from acidic soils (*i.e.* soils with pH <6.3) and consistently occur on soils with relatively high DTPA-extractable Ca, Mg and Ni concentrations (van der et al., 2016c). It appears that the very high extractability of Ni in the soils were more important than pH conditions for Ni hyperaccumulators. With the exception of the soil at Sake South, the situation at Weda Bay was similar to that of Sabah, with all Ni hyperaccumulators occurring on eroded hypermagnesic Cambisols with (extremely) high DTPA-extractable Ni concentration. These shallow hypermagnesic Cambisols host a xerophytic adapted vegetation in which Ni hyperaccumulators were common, and this aligns with reports from other tropical ultramafic regions, for example in Cuba, New Caledonia, Sabah and the Philippines (van der Ent et al., 2016a).

In contrast, Geric Ferralsols such as at Uni-Uni plot 2, or Bukit Limber plots 1 and 2 have no occurrence of Ni hyperaccumulators and this may be explained by their physico-chemical characteristics: these soils had low DTPA-extractable Ni concentration, acidic pH, and a mineralogy dominated by goethite and hematite which resulted in a very low CEC. However, the DTPA-extractable Al in these soils was high (up to 45 mg $kg^{-1}$) although ultramafic bedrocks are relatively poor in Al, and these soils host Al hyperaccumulators from families or groups that were previously known to contain Al hyperaccumulator taxa in nearby tropical regions: *e.g.* three

449 different species of *Symplocos* (Symplocaceae), one species of *Syzygium* (Myrtaceae), one species
450 of *Melastoma* (Melastomataceae), one species of *Psychotria* (Rubiaceae), and several species from
451 the Lauraceae, Theaceae and Cunoniaceae families. Therefore, Ni and Al hyperaccumulation were
452 found in contrasted edaphic situations which was confirmed by the foliar chemistry data from Weda
453 Bay, but also from nearby Sabah (van der Ent et al., 2018b).
454
455 Laboratory analysis with ICP-AES confirmed the indicative results achieved from the initial testing
456 in the field with DMG-test paper. Field-testing with DMG paper therefore remains a reliable and
457 quick method for Ni hyperaccumulator reconnaissance. After analysis, the highest Ni
458 concentrations in hyperaccumulator leaves were found in the shrub *R.* aff. *bengalensis* and in the
459 tree *P. roxburghiana*. Both species were hypernickelophores (with foliar Ni concentrations usually
460 above 1.0 %) and were only reported in soils with high DTPA-extractable Ni. In total four species
461 from the 18 hyperaccumulators reported could be considered as metal crops (high biomass, high Ni
462 accumulation), these were: *R.* aff. *bengalensis, F. trachypison, T. morotaiense* and *G. moluccanum*.
463 Of these species, *F. trachypison, T. morotaiense* and *G. moluccanum* appeared to be facultative Ni
464 hyperaccumulator species and pioneer species suitable for first-phase implementation on minerals
465 waste. *Rinorea* aff. *bengalensis,* is a strong Ni hyperaccumulator and could be cropped as an
466 understory shrub under the cover of species such as *T. morotaiense* in the second stage of
467 agromining and then coppiced for efficient Ni phytoextraction.
468
469 From the plants collected at Weda Bay, two specimens of *R.* aff. *bengalensis* showed Co
470 hyperaccumulation. Both were collected at the location 'Tanjung Ulie'. High foliar Co
471 concentrations had already been reported in the strong Ni hyperaccumulators *Rinorea javanica*
472 (Violaceae) with up to 670 μg $g^{-1}$ in natural conditions (Brooks et al., 1977; Lange et al., 2017). The
473 strong affinity of Mn-oxides for Co may explain the lower Co mobility in Mn-rich soils (Collins
474 and Kinsela, 2011). When soils are waterlogged, Co is associated mainly with amorphous Fe oxides
475 after the reduction of Mn and the dissolution of Mn-oxides, and thus becomes more available
476 (Lange et al., 2017). These conditions are also responsible for the high Co concentrations observed
477 in some *Rinorea* species as observed for other species, such as *Berkheya coddii* in South Africa
478 (Lange et al., 2017).
479
480 The occurrence of parasitic mistletoes on hyperaccumulator plants is a very rare phenomenon, and
481 has not previously been reported in tropical species or woody hyperaccumulator plants/mistletoes.
482 The herbaceous *Orobanche nowackiana* parasitizes the Ni hyperaccumulator *Alyssum murale* in
483 Albania while accumulating up to 299 mg $kg^{-1}$ in its leaves (Bani et al., 2018). Similarly, Reeves

(1992) reported *O. rechingeri* parasitizing *Alyssum lesbiacum* while accumulating more than 600 mg $kg^{-1}$ Ni. The only other now example is the American *Cuscuta californica* parasitizing the herbaceous Ni hyperaccumulator *Streptanthus polygaloides* reaching up to 800 mg $kg^{-1}$ Ni (Boyd et al., 1999).

With only a small portion of the ultramafic flora of Indonesia screened for Ni hyperaccumulation, this field survey considerably extends the list of Indonesian Ni hyperaccumulators. It is expected that more Ni hyperaccumulators will be discovered in the near future in this country because it has the largest ultramafic extension worldwide with a highly diverse flora (van der Ent et al., 2013b). Many hyperaccumulator plants are rare, with restricted ranges on ultramafic soils, making them sensitive to destructive forces of mining and forest fires (Whiting et al., 2004; Erskine et al., 2012), and this adds to the urgency for screening to avoid this valuable biological resource from being lost before its known.

**ACKNOWLEDGEMENTS**

We acknowledge the financial and operational support from Eramet and PT Weda Bay Nickel to conduct this research. The French National Research Agency through the national "Investissements d'avenir" program (ANR-10-LABX-21, LABEX RESSOURCES21) and through the ANR-14-CE04-0005 Project "Agromine" is acknowledged for funding support. PT Weda Bay Nickel were responsible for all relevant permits in Indonesia and for transporting the plant and soil samples for chemical analysis in France. A. van der Ent is the recipient of a Discovery Early Career Researcher Award (DE160100429) from the Australian Research Council.

**REFERENCES**

Baker, A.J.M. 1981. Accumulators and excluders -strategies in the response of plants to heavy metals. Journal of Plant Nutrition 3, 643–654. doi:10.1080/01904168109362867

Baker, A.J.M. 1987. Metal tolerance. New Phytologist 106, 93–111.

Baker, A.J.M., Brooks, R.R. 1989. Terrestrial higher plants which hyper accumulate metallic elements. Biorecovery 1, 81–126.

Bani, A., Pavlova, D., Benizri, E., Shallari, S., Miho, L., Meco, M., Shahu, E., Reeves, R., Echevarria, G., 2018. Relationship between the Ni hyperaccumulator *Alyssum murale* and the

518 parasitic plant *Orobanche nowackiana* from serpentines in Albania. Ecological Research
519 33(3):549–559.
520
521 Barbaroux, R., Mercier, G., Blais, J.F., Morel, J.L., Simonnot, M.O. 2011. A new method for
522 obtaining nickel metal from the hyperaccumulator plant *Alyssum murale*. Separation and
523 Purification Technology 83, 57–65.
524
525 Bouman, R., van Welzen. P.W., Sumail, S., Echevarria, G., Erskine, P.D., van der Ent A. 2018.
526 *Phyllanthus rufuschaneyi*: a new nickel hyperaccumulator from Sabah (Borneo Island) with
527 potential for tropical agromining. Botanical Studies 59, 9. DOI: 10.1186/s40529-018-0225-y
528
529 Boyd, R.S., Martens, S.N. 1998. The significance of metal hyperaccumulation for biotic
530 interactions. Chemoecology 8, 1–7.
531
532 Boyd, R.S., Martens N. S., Davis M.A. 1999l. The nickel hyperaccumulator *Streptanthus*
533 *polygaloides* (Brassicaceae) is attacked by the parasitic plant *Cuscuta californica* (Cuscutaceae).
534 Madrono 46:92–99
535
536 Brooks, R.R. 1987. Serpentine and its vegetation: a multidisciplinary approach, Dioscorides Press,
537 462 pp.
538
539 Brooks, R.R., Wither, E.D., Zepernick, B. 1977. Cobalt and nickel in *Rinorea* species. Plant and
540 Soil 47(3), 707–712.
541
542 Butt, C.R.M., Cluzel, D. 2013. Nickel laterite ore deposits: weathered serpentinites. Elements 9 (2),
543 123–128.
544
545 Chaney, R.L., Angle, J.S., Broadhurst, C.L., Peters, C.A., Tappero, R.V., Sparks, D.L. 2007.
546 Improved Understanding of Hyperaccumulation Yields Commercial Phytoextraction and
547 Phytomining Technologies. Journal of Environmental Quality 36, 1429–1443.
548
549 Chaney, R. 1983. Plant uptake of inorganic waste constitutes. Land Treatment of Hazardous
550 Wastes, 50–76.
551
552 Chenery, E.M. 1949. Aluminium in the plant world. Kew Bulletin 4, 463. doi:10.2307/4109057

Collins, R.N., Kinsela, A.S. 2011. Pedogenic factors and measurements of the plant uptake of cobalt. Plant and Soil 339, 499–512.

Davis C.C., Webb, C.O., Wurdack, K.J., Jaramillo, C.A., Donoghue M.J. 2005. Explosive Radiation of Malpighiales Supports a Mid-Cretaceous Origin of Modern Tropical Rain Forests. The American Naturalist 165, 3 – E36-E65.

Echevarria, G. 2018. Genesis and behaviour of ultramafic soils and consequences for nickel biogeochemistry. In: van der Ent, A., Echevarria, G., Baker, A.J.M., Morel, J.L. (Eds.), Agromining: Extracting Unconventional Resources from Plants, Mineral Resource Reviews Series. SpringerNature, pp 135–156.

Erskine, P.D., Van der Ent, A., Fletcher, A. 2012. Sustaining metal-loving plants in mining regions. Science 337, 1172–1173.

Galey, M.L., van der Ent, A., Iqbal, M.C.M, Rajakaruna, N. 2017. Ultramafic geoecology of South and Southeast Asia. Botanical Studies 58, 18. doi: 10.1186/s40529-017-0167-9

Guillot, S., Hattori, K. 2013. Serpentinites: essential roles in geodynamics, arc volcanism, sustainable development, and the origin of life. Elements 9 (2), 95–98.

Jaffré, T., Pillon, Y., Thomine, S., Merlot, S. 2013. The metal hyperaccumulators from New Caledonia can broaden our understanding of nickel accumulation in plants. Frontiers in Plant Science 4, 279.

Jaffré, T., Reeves R.D., Baker A.J.M., van der Ent, A. 2018. The discovery of nickel hyperaccumulation in the New Caledonian tree *Pycnandra acuminata*: 40 years on. New Phytologist 218: 397–400.

Kitayama, K., Majalap-Le, N., Aiba, S. 2000. Soil phosphorus fractionation and phosphorus-use efficiencies of tropical rainforests along altitudinal gradients of Mount Kinabalu, Borneo. Oecologia 123, 342–349.

587 Korotkova, N., Schneider, J.V., Quandt, D. Worberg A., Zizka, G., Borsch. T. 2009. Phylogeny of
588 the eudicot order Malpighiales: analysis of a recalcitrant clade with sequences of the petD group II
589 intron. Plant Systematics and Evolution 282(3–4), 201–228.
590
591 Kostermans, A. 1972. A synopsis of the Old World species of *Trichospermum* Blume (Tiliaceae).
592 Transactions of the Botanical Society of Edinburgh 41, 401–430.
593
594 Lange, B., van der Ent, A., Baker, A.J.M., Mahy, G., Malaisse, F., Meerts, P., Echevarria, G.,
595 Pourré, O., Verbruggen, N., Faucon, M.P. 2017. Copper and cobalt accumulation in plants: a
596 critical assessment of the current status of knowledge. New Phytologist 213 (2), 537–551.
597
598 Lindsay, W.L., Norvell, W.A. 1978. Development of DTPA soil test for zinc, iron, manganese, and
599 copper. Soil Science Society of America Journal 42, 421–428.
600
601 Lopez S., Goux X., van der Ent A., Erskine P.D., Echevarria G., Calusinska M., Morel JL., Benizri,
602 E. 2019a. Bacterial community diversity in the rhizosphere of nickel hyperaccumulator species of
603 Halmahera Island (Indonesia). Applied Soil Ecology 133, 70–80.
604
605 Lopez S., van der Ent A., Erskine P.D., Echevarria G, Morel JL., Lee G., Permana E., Benizri, E.
606 2019b. Rhizosphere chemistry and above-ground elemental fractionation of nickel
607 hyperaccumulator species from Weda Bay (Indonesia). Plant and Soil. Under review.
608
609 Martens, S.N., Boyd, R.S. 1994. The ecological significance of nickel hyperaccumulation: a plant
610 chemical defense. Oecologia 98, 379–384.
611
612 Mesjasz-Przybylowicz, J., Przybylowicz, W., Barnabas, A., van der Ent, A. 2016. Extreme nickel
613 hyperaccumulation in the vascular tracts of the tree *Phyllanthus balgooyi* from Borneo. New
614 Phytologist 209, 1513–1526.
615
616 Nkrumah, P., Echevarria, G., Erskine, P.D., van der Ent, A. 2018. The discovery of nickel hyper-
617 accumulation in *Antidesma montis-silam*: from herbarium identification to field re-discovery.
618 Ecological Research. 33(3), 675–685.
619
620 Pollard, A.J, Reeves, R.D, Baker, A.J.M. 2014. Facultative hyperaccumulation of heavy metals and
621 metalloids. Plant Science 217–218, 8–17.

Proctor, J. 2003. Vegetation and soil and plant chemistry on ultramafic rocks in the tropical Far East. Perspectives in Plant Ecol 6(1–2), 105–124.

Rajakaruna, N. Baker, A. J. M., 2004. Serpentine: a model habitat for botanical research in Sri Lanka. Ceylon Journal of Science. 32, 1–19.

Reeves. R.D. 1992. The hyperaccumulation of nickel by serpentine plants. In: Baker AJM, Proctor J, Reeves RD (eds) The vegetation of ultramafic (Serpentine) Soils. Intercept Ltd., Andover, pp 253–277

Reeves, R. D. 2006. Hyperaccumulation of trace elements by plants. Phytoremediation of metal-contaminated soils, Morel, JL, Echevarria, G, Goncharova, N (Eds.), pp 25–52.

Reeves, R.D. 2003. Tropical hyperaccumulators of metals and their potential for phytoextraction. Plant and Soil 249(1), 57–65

Reeves, R.D., Baker, A.J.M, Borhidi, A., Berazaín, R. 1999. Nickel hyperaccumulation in the serpentine flora of Cuba. Annals of Botany 83(1), 1–10.

Reeves, R.D., Baker, A.J.M., Borhidi, A., Berazaín, R. 1996. Nickel-accumulating plants from the ancient serpentine soils of Cuba. New Phytologist 133(2), 217–224.

Reeves, R.D., Baker, A.J.M., Jaffré, T., Erskine, P.D., Echevarria, G., van der Ent, A. 2018a. A global database for hyperaccumulator plants of metal and metalloid trace elements. New Phytologist 218: 397–400.

Reeves, R.D., van der Ent A., Baker, A.J.M. 2018b. Global distribution and ecology of hyperaccumulator plants. In: "Agromining: extracting unconventional resources from plants, " Mineral Resource Reviews series, Van der Ent, A., Echevarria, G., Baker, A.J.M., Morel, J.L (Eds.), SpringerNature, pp 75–92.

Schmitt, M., Boras, S., Tjoa, A., Watanabe, T., Jansen, S., 2016. Aluminium Accumulation and Intra-Tree Distribution Patterns in Three *Arbor aluminosa* (*Symplocos*) Species from Central Sulawesi. PLoS ONE 11, e0149078–18. doi:10.1371/journal.pone.0149078

Searle, M.P., Stevens, R.K. 1984. Obduction processes in ancient, modem and future ophiolites. In: Gass, I.G., Lippard, S.J., Shelton, A.W. (Eds.), Ophiolites and Oceanic Lithosphere. Blackwell, London, pp. 303–319.

van der Ent, A., Mulligan, D. R. 2015. Multi-element concentrations in plant parts and fluids of Malaysian nickel hyperaccumulator plants and some economic and ecological considerations. J Chem Ecol 41, 396–408.

van der Ent, A., Baker, A.J.M., Reeves, R.D., Pollard, A.J., Schat, H. 2013a. Hyperaccumulators of metal and metalloid trace elements: Facts and fiction. Plant and Soil 362, 319–334.

van der Ent, A., Baker, A.J.M., van Balgooy, M.M.J., Tjoa, A. 2013b. Ultramafic nickel laterites in Indonesia (Sulawesi, Halmahera): Mining, nickel hyperaccumulators and opportunities for phytomining. Journal of Geochemical Exploration 128, 72–79.

van der Ent, A., Erskine, P.D., Sumail, S. 2015b. Ecology of nickel hyperaccumulator plants from ultramafic soils in Sabah (Malaysia). Chemoecology 25, 243–259.

van der Ent, A., Baker, A. J. M., Reeves, R.D., Chaney, R. L., Anderson, C. W. N., Meech, J. A., Erskine, P. D., Simonnot, M. O., Vaughan, J., Morel, J. L., Echevarria, G., Fogliani, B., Qiu, R.-L., Mulligan, D. 2015a. Agromining: farming for metals in the future? Environ Sci and Technol 49, 4773–4780.

van der Ent, A., Echevarria, G., Tibbett, M. 2016a. Delimiting soil chemistry thresholds for nickel hyperaccumulator plants in Sabah (Malaysia). Chemoecology 26, 67–82.

van der Ent A., Erskine, P.D., Mulligan, D.R, Repin, R., Karim, R. 2016b. Vegetation on ultramafic edaphic 'islands' in Kinabalu Park (Sabah, Malaysia) in relation to soil chemistry and elevation. Plant and Soil 403, 77–101.

van der Ent A., van Balgooy M., van Welzen, P. 2016c. *Actephila alanbakeri* (Phyllanthaceae): a new nickel hyperaccumulating plant species from localised ultramafic outcrops in Sabah (Malaysia). Botanical Studies 57, 19.

van der Ent, A., Callahan, D.L., Noller, B.N., Mesjasz-Przybylowicz, J., Przybylowicz, W.J., Barnabas, A., Harris, H.H. 2017. Nickel biopathways in tropical nickel hyperaccumulating trees from Sabah (Malaysia). Scientific Reports 7, srep41861.

van der Ent, A., Przybyłowicz W.J., de Jonge M.D., Harris H.H., Ryan C.G., Tylko, G., Paterson D.J., Barnabas, A.D., Kopittke, P.M., Mesjasz-Przybyłowicz, J. 2017. X-ray elemental mapping techniques for elucidating the ecophysiology of hyperaccumulator plants. New Phytologist 218, 432–452. doi: 10.1111/nph.14810

van der Ent, A., Cardace, D., Tibbett, M., Echevarria, G. 2018a. Ecological implications of pedogenesis and geochemistry of ultramafic soils in Kinabalu Park (Malaysia). Catena 160, 154–169.

van der Ent A., Mulligan D.R., Repin R., Erskine P.D. 2018b. Foliar elemental profiles in the ultramafic flora of Kinabalu Park (Sabah, Malaysia). Ecological Research 33(3), 659–674.

Vitousek, P.M., Sanford, R.L. 1983. Nutrient cycling in moist tropical forest. Annual Review of Ecology and Systematics 17, 137–167.

Vitousek, P.M., Porder, S., Houlton, B.Z., Chadwick, O.A. 2010. Terrestrial phosphorus limitation: mechanisms, implications, and nitrogen-phosphorus interactions. Ecological applications: a publication of the Ecological Society of America 20, 5–15.

Whiting, S., Reeves, R.R., Richards, D, Johnson, M., Cooke, J., Malaisse, F., Paton, A., Smith, J., Angle, J., Chaney, R.L., et al. 2004. Research priorities for conservation of metallophyte biodiversity and their potential for restoration and site remediation. Restoration Ecology 12, 106–116.

Wither, E.D., Brooks, R.R. 1977. Hyperaccumulation of nickel by some plants of Southeast Asia. Journal of Geochemical Exploration 8(3), 579–583

724 **FIGURE CAPTIONS**

725

726 **Figure 1**. Map of the field sampling sites and the location of Weda Bay on Halmahera Island,
727 Indonesia.

728

729 **Figure 2.** Aerial views of the landscapes at Weda Bay, Halmahera, Indonesia. Panel **A** shows
730 exposed serpentinite bedrock in a rock fall near Jira with forest dominated by Casuarinaceae; panel
731 **B** showing a riverbed upstream of the site of panel A with serpentinite bedrock and a short scrubby
732 vegetation; Panel **C** shows mature riverine further downstream; panel **D** shows burnt vegetation on
733 Plinthic Geric Rhodic Ferralsols near Uni-Uni.

734

735 **Figure 3.** Ground-level views of vegetation types at Weda Bay, Halmahera, Indonesia. Panel **A**
736 shows mature riverine forest at the site "Serpentinite River"; panel **B** shows mature forest near site
737 Casuarina' panel **C** shows burnt 'maquis-type' vegetation characterised by sedges (Cyperaceae) on
738 Geric Plinthic Rhodic Ferralsols at Uni-Uni, and panel **D** shows young forest dominated by
739 *Macaranga* spp. (Euphorbiaceae) on Ferralic Rhodic Hypereutric Cambisols (Hypermagnesic) at
740 Sake River.

741

742 **Figure 4.** Soil profiles at key localities at Weda Bay, Halmahera, Indonesia. Panel **A** shows
743 Hypereutric Cambic Skeletic Leptosols (Hypermagnesic) at the site "Blue Hill"; panel **B** shows
744 Geric Plinthic Rhodic Ferralsols; panel **C** shows ferrocrete with plinthic nodules consisting mainly
745 of hematite; panels **D** and **E** show Hypereutric Cambisols (Hypermagnesic) at the sites Casuarina
746 and Sake West; panel **F** shows Geric Plinthic Rhodic Ferralsols at Uni-Uni.

747

748 **Figure 5.** X-Ray Diffractograms of the fine earth fraction (< 50 mm) of the B horizons of 5
749 representative profiles on ultramafic bedrock and of the A-organo-mineral horizon of the Rendzic
750 Leptosol on Limestone. CALC=Calcite; DIOP=Diopside; ENST=Enstatite; GIBBS=Gibbsite;
751 GOET=Goethite; HEM=Hematite; MAGN=Magnetite; QUARTZ=Quartz; TREM=Tremolite;
752 SERP=Serpentine.

753

**Figure 6.** Plant part and soil total concentrations of different elements for non-hyperaccumulator plants (**A**) and hyperaccumulator plants (**B**). All concentrations are expressed as mg $kg^{-1}$ dry mass.

**Figure 7.** Correlations between element concentrations in plant parts (natural logarithm scale) and number of hyperaccumulator (93 samples) and non-hyperaccumulator (724 samples) plants.

**Figure 8.** Plant foliar and soil bioavailable concentrations with DTPA extractions of different elements for non-hyperaccumulator plants and hyperaccumulator plants. All concentrations are expressed as mg $kg^{-1}$ dry mass.

**Figure 9.** The mistletoe *Amyema cuernosensis* parasitizing the Ni hyperaccumulator *Ficus trachypison* near the Casuarina site. Panel **A** shows the while mistletoe plant attached to the host; panel **B** shows the inflorescences of *Amyema cuernosensis;* and Panel **C** shows a section of woody stem of *Ficus trachypison* with the mistletoe stems attached with haustoria.

## TABLE CAPTIONS

**Table 1**. Sites properties showing plot enumeration, location, soil class and dominant vegetation type.

**Table 2.** Mineralogy of the soils (Mineral horizons – 10–25 cm layer) sampled at each site. For the soil in Doromesmesan, the mineralogy was based on the organo-mineral Horizon (0-5 cm layer). +++ (most abundant mineral); ++ (abundant mineral); + (frequent mineral); (+) (detectable traces).

**Table 3**. Total elements for mineral soil (10–25 cm layer) samples from each site.

**Table 4.** Total elements for organo-mineral soil (0–5 cm layer) samples from each site.

**Table 5.** DTPA-extractable elements for mineral soil (10–25 cm layer) samples from each site.

**Table 6.** DTPA-extractable elements for organo-mineral soil (0–5 cm layer) samples from each site.

**Table 7.** pH, exchangeable cations ($cmol^+ kg^{-1}$) and nitrogen and carbon content for mineral soil (10–25 cm layer) samples from each site. Abbreviations: Cation Exchange Capacity (CEC), % of soil total nitrogen (%N), % of soil total carbon (%C), % of soil organic carbon (%Corg).

**Table 8.** pH, exchangeable cations ($cmol^+ kg^{-1}$) and nitrogen and carbon content for organo-mineral soil (0–5 cm layer) samples from each site. Abbreviations: Cation Exchange Capacity (CEC), % of soil total nitrogen (%N), % of soil total carbon (%C), % of soil organic carbon (%Corg).

**Table 9.** Ni distribution in leaf samples ($mg\ kg^{-1}$) and soil samples for each site. Abbreviations: Extractable Ni (Ni-DTPA, $mg\ kg^{-1}$), Exchangeable Ni (Ni-CEC, $cmol+\ kg^{-1}$) and Ni total (Ni-T, $g\ kg^{-1}$), no data (n.d).

**Table 10.** Aluminium ($mg\ kg^{-1}$) hyperaccumulator plant records (identified and unidentified specimens) from the Weda Bay area.

**Table 11.** Elemental concentrations ($mg\ kg^{-1}$) in the mistletoe *Amyema cuernosensis* (Loranthaceae) and the host *Ficus trachypison* (Moraceae).

**SUPPLEMENTARY INFORMATION**

**Table S1.** Macronutrients (g $kg^{-1}$) of non-hyperaccumulator leaves (number of samples are indicated, means and ranges are provided).

**Table S2.** Micronutrients (mg $kg^{-1}$) of non-hyperaccumulator leaves (number of samples are indicated, means and ranges are provided).

**Table S3.** Macronutrients (g $kg^{-1}$) of hyperaccumulator leaves (number of samples are indicated, means and ranges are provided).

**Table S4.** Micronutrients (mg $kg^{-1}$) of hyperaccumulator leaves (number of samples are indicated, means and ranges are provided).

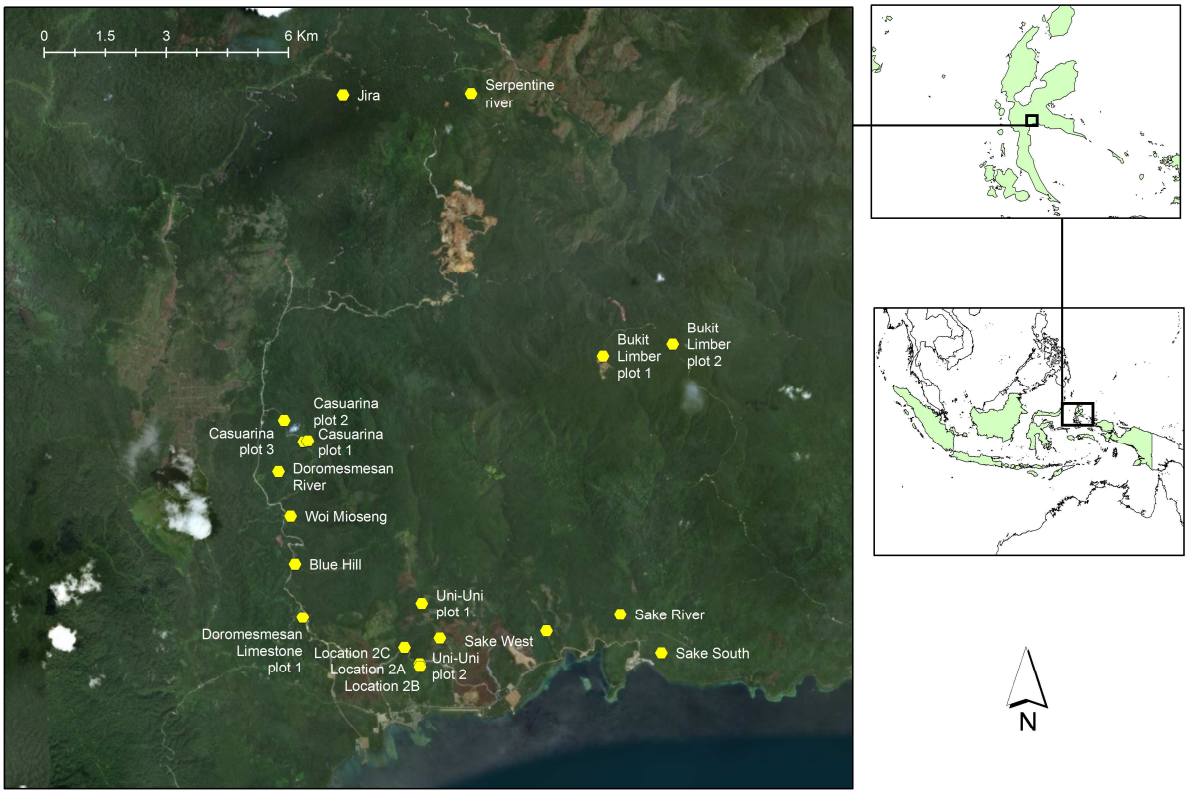


1

2

3 **Figure 1**. Map of the field sampling sites and the location of Weda Bay on Halmahera Island,

4 Indonesia.

5

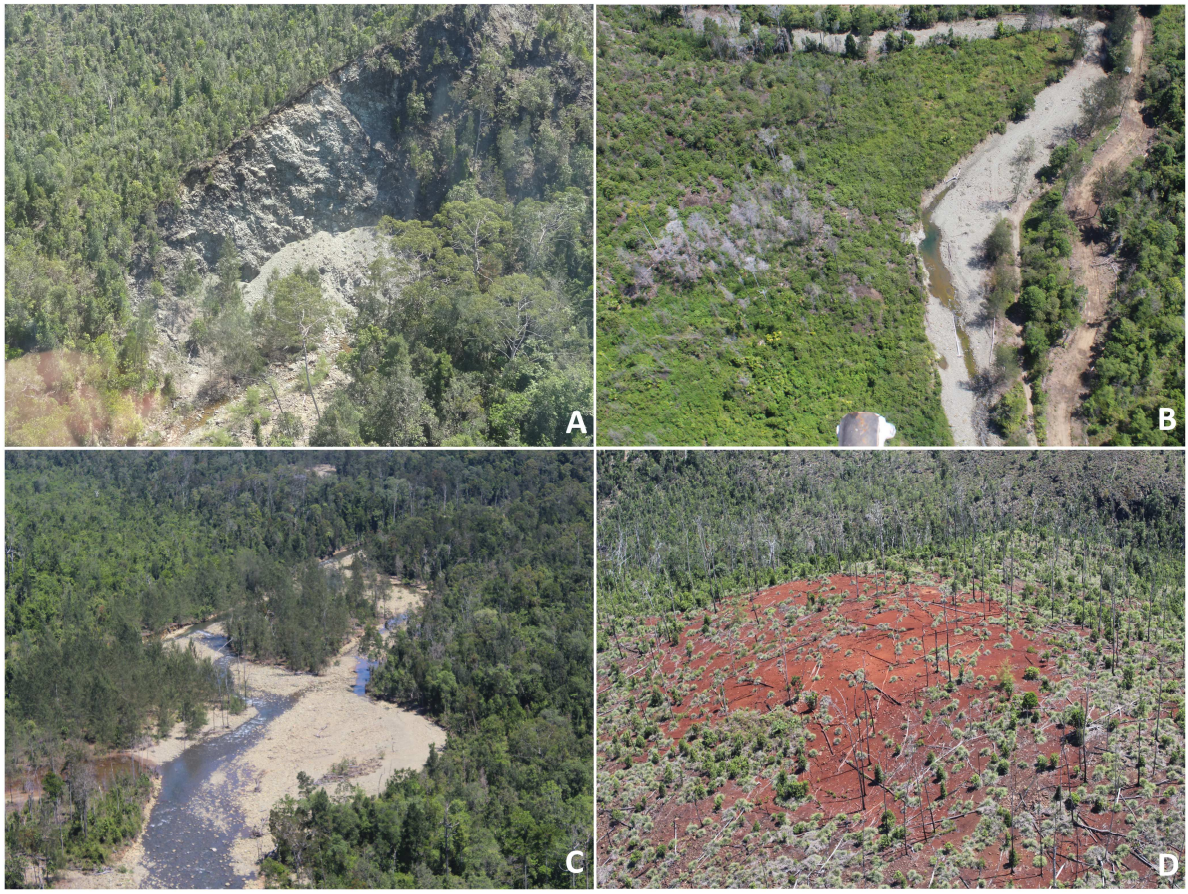


**Figure 2.** Aerial views of the landscapes at Weda Bay, Halmahera, Indonesia. Panel **A** shows exposed serpentinite bedrock in a rock fall near Jira with forest dominated by Casuarinaceae; panel **B** showing a riverbed upstream of the site of panel A with serpentinite bedrock and a short scrubby vegetation; Panel **C** shows mature riverine further downstream; panel **D** shows burnt vegetation on Plinthic Geric Rhodic Ferralsols near Uni-Uni.


**Figure 3.** Ground-level views of vegetation types at Weda Bay, Halmahera, Indonesia. Panel **A** shows mature riverine forest at the site "Serpentinite River"; panel **B** shows mature forest near site Casuarina' panel **C** shows burnt 'maquis-type' vegetation characterised by sedges (Cyperaceae) on Geric Plinthic Rhodic Ferralsols at Uni-Uni, and panel **D** shows young forest dominated by *Macaranga* spp. (Euphorbiaceae) on Ferralic Rhodic Hypereutric Cambisols (Hypermagnesic) at Sake River.

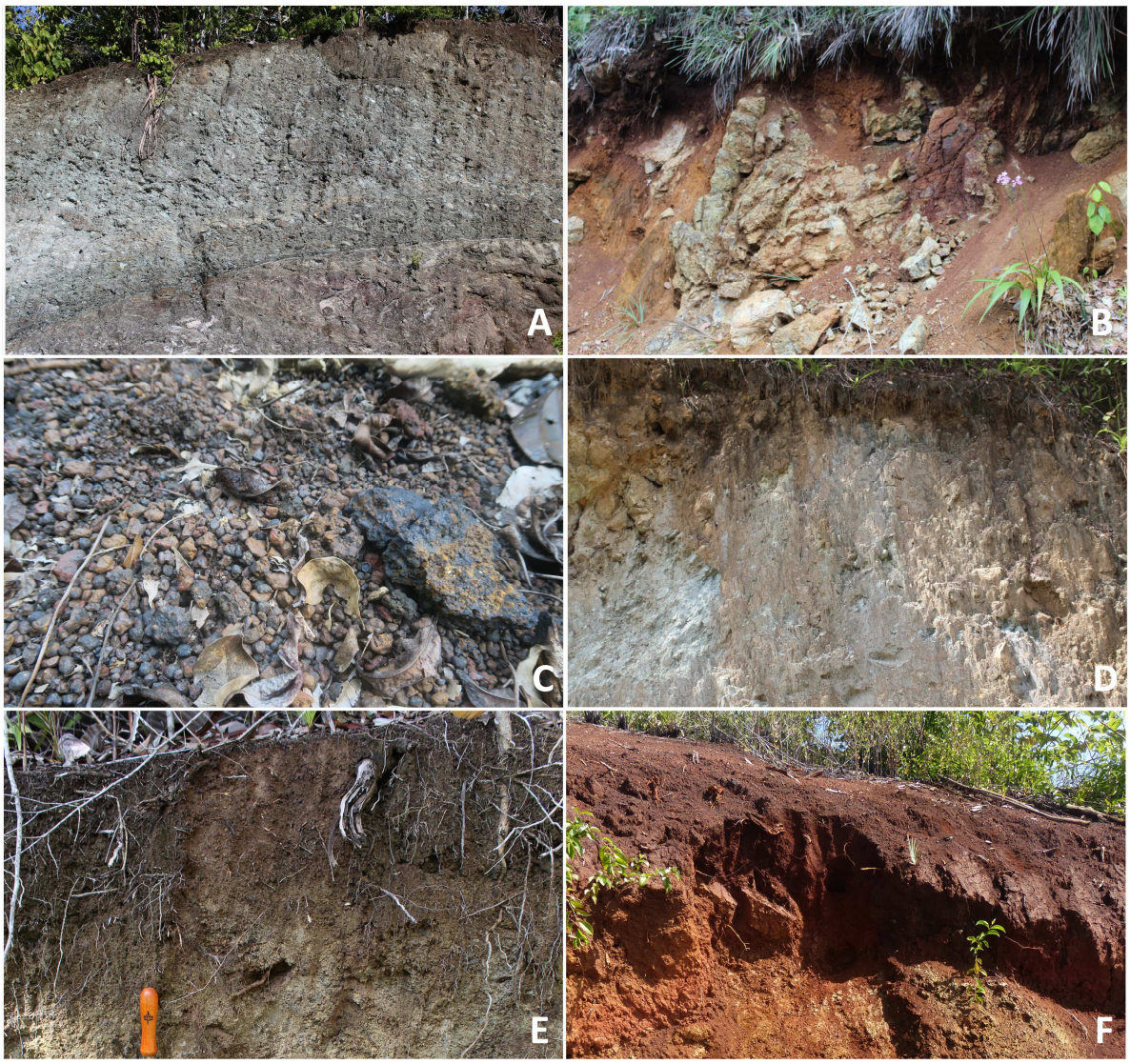


**Figure 4.** Soil profiles at key localities at Weda Bay, Halmahera, Indonesia. Panel **A** shows Hypereutric Cambic Skeletic Leptosols (Hypermagnesic) at the site "Blue Hill"; panel **B** shows Geric Plinthic Rhodic Ferralsols; panel **C** shows ferrocrete with plinthic nodules consisting mainly of hematite; panels **D** and **E** show Hypereutric Cambisols (Hypermagnesic) at the sites Casuarina and Sake West; panel **F** shows Geric Plinthic Rhodic Ferralsols at Uni-Uni.

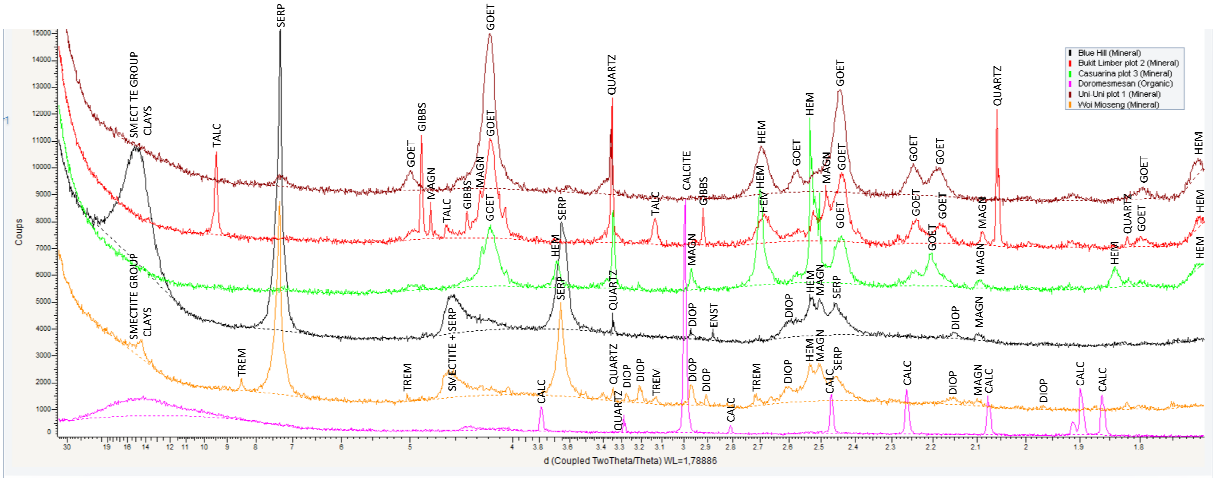


**Figure 5.** X-Ray Diffractograms of the fine earth fraction (< 50 mm) of the B horizons of 5 representative profiles on ultramafic bedrock and of the A-organo-mineral horizon of the Rendzic Leptosol on Limestone. CALC=Calcite; DIOP=Diopside; ENST=Enstatite; GIBBS=Gibbsite; GOET=Goethite; HEM=Hematite; MAGN=Magnetite; QUARTZ=Quartz; TREM=Tremolite; SERP=Serpentine.

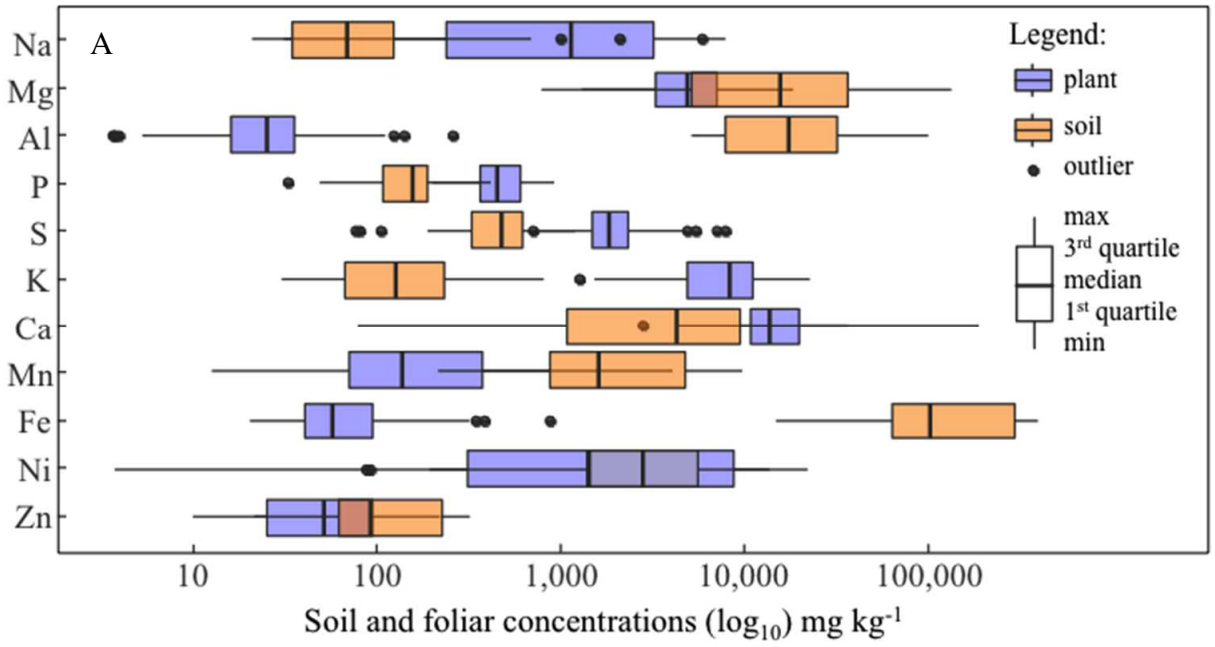


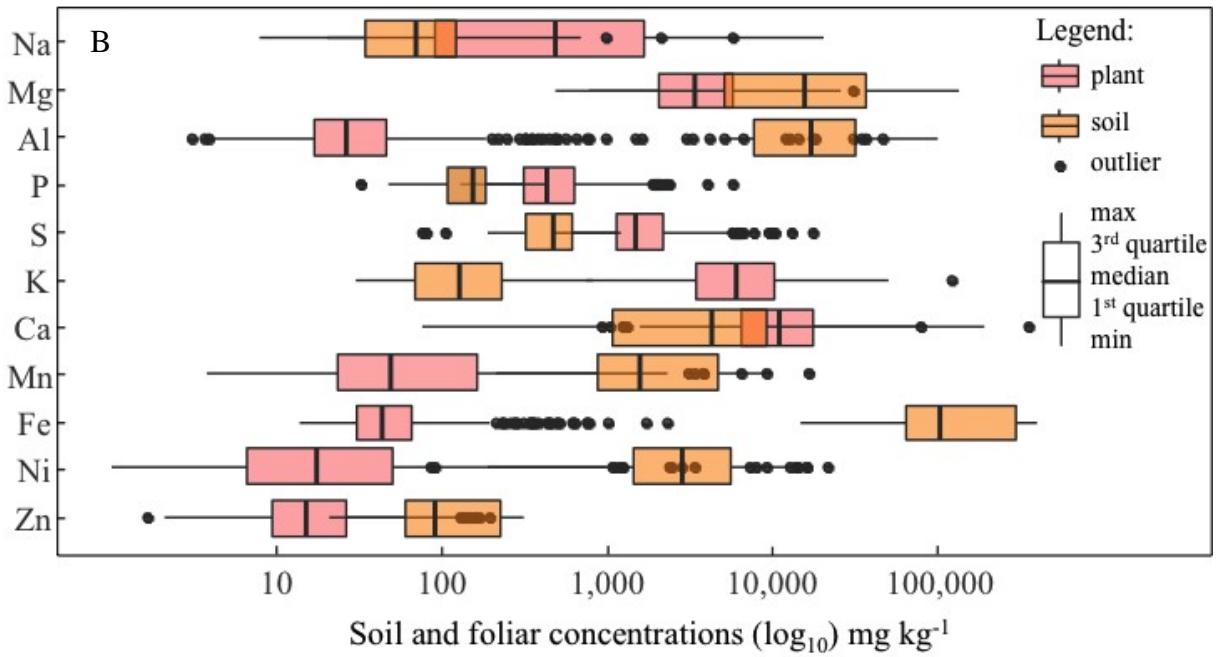


**Figure 6.** Plant part and soil total concentrations of different elements for non-hyperaccumulator plants (**A**) and hyperaccumulator plants (**B**). All concentrations are expressed as mg $kg^{-1}$ dry mass.

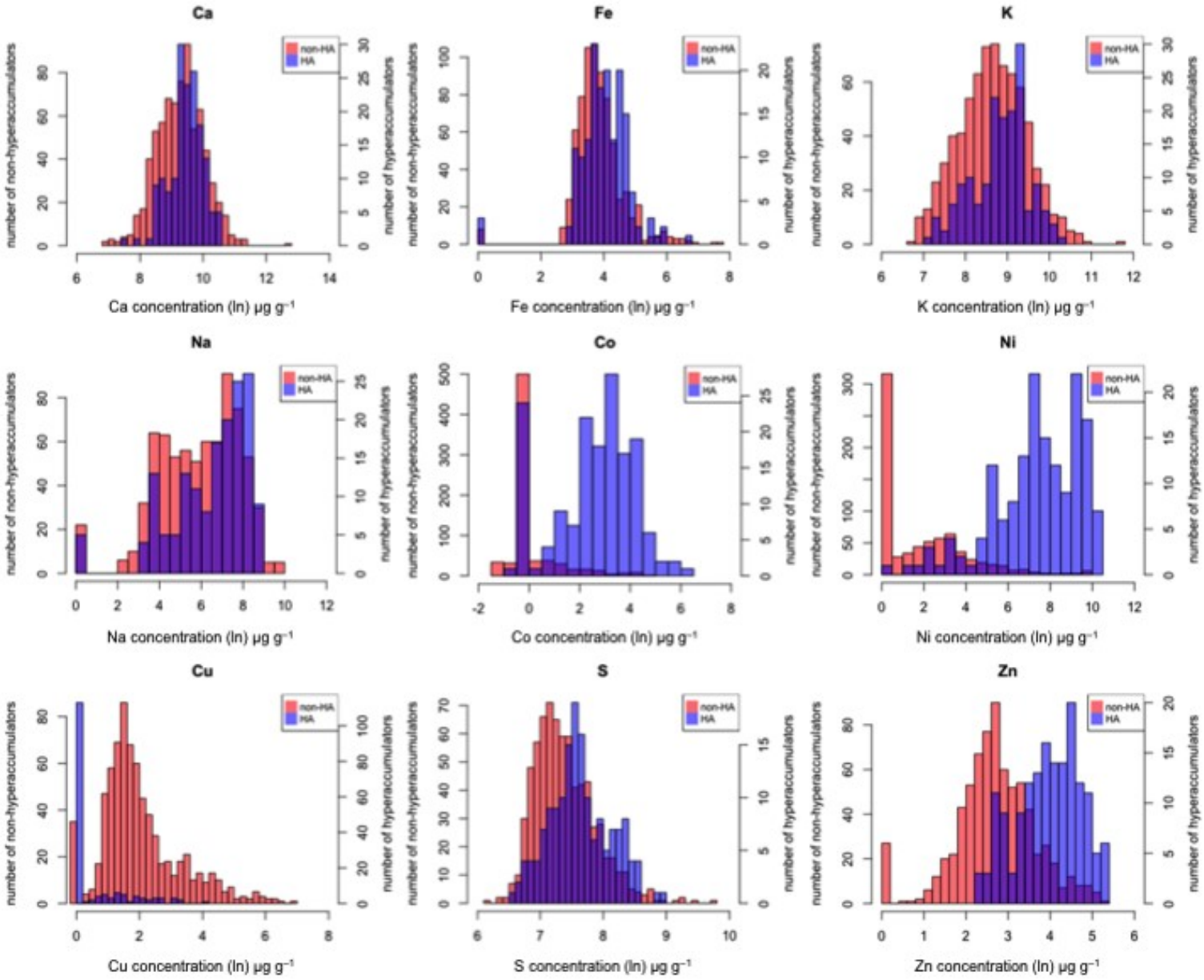


**Figure 7.** Correlations between element concentrations in plant parts (natural logarithm scale) and number of hyperaccumulator (93 samples) and non-hyperaccumulator (724 samples) plants.

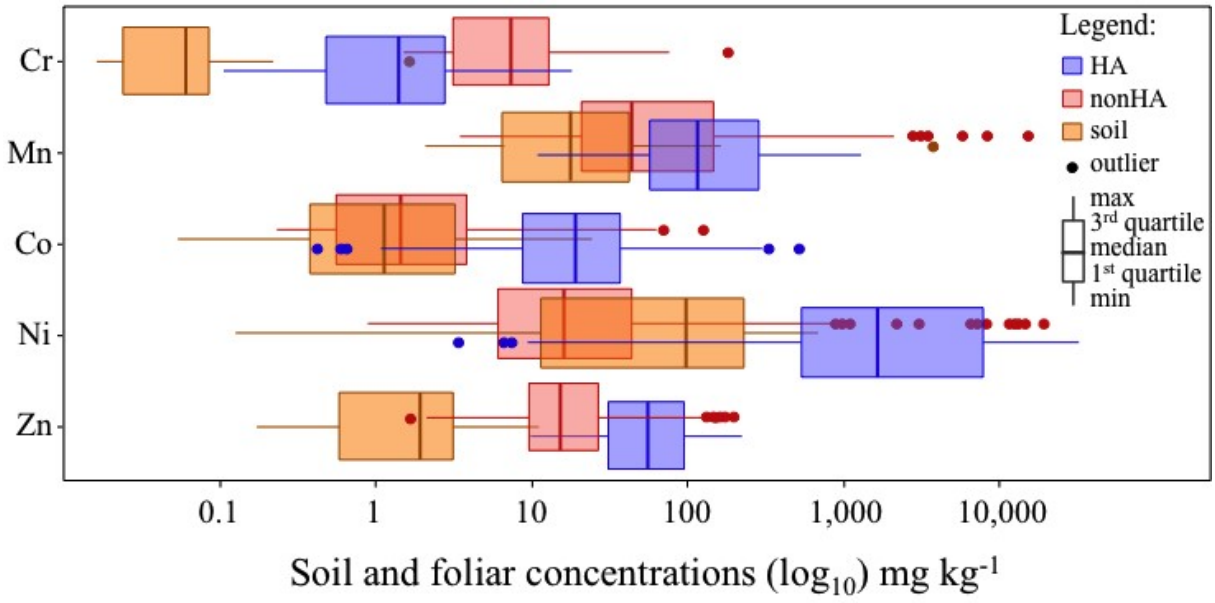


**Figure 8.** Plant foliar and soil bioavailable concentrations with DTPA extractions of different elements for non-hyperaccumulator plants and hyperaccumulator plants. All concentrations are expressed as mg $kg^{-1}$ dry mass.


**Figure 9.** The mistletoe *Amyema cuernosensis* parasitizing the Ni hyperaccumulator *Ficus trachypison* near the Casuarina site. Panel **A** shows the while mistletoe plant attached to the host; panel **B** shows the inflorescences of *Amyema cuernosensis;* and Panel **C** shows a section of woody stem of *Ficus trachypison* with the mistletoe stems attached with haustoria.

| Sites | Plot | Elevation (m asl) | GPS coordinates | Soil class | Vegetation type |
|---|---|---|---|---|---|
| Bukit Limber | Plot 1 | 909 | 0°32'49"N, 127°58'35"E | Rhodic Plinthic Ferralsol (Hypereutric, Hypermagnesic) | Lower montane forest |
| | Plot 2 | 1020 | 0°32'58"N, 127°59'31"E | Geric Rhodic Plinthic Ferralsol (Magnesic) | Lower montane forest |
| Casuarina | plot 1 | 189 | 0°31'41"N, 127°54'37"E | Leptic Hypereutric Rhodic Cambisol (Magnesic) | Medium tall lowland forest |
| | plot 2 | 190 | 0°31'41"N, 127°54'40"E | Leptic Hypereutric Rhodic Cambisol (Magnesic) | Medium tall lowland forest |
| | plot 3 | 204 | 0°31'57"N, 127°54'22"E | Rhodic Plinthic Mollic Ferralsol (Dystric, Magnesic) | Medium tall lowland forest |
| Doromesmesan Limestone | plot 1 | 73 | 0°29'20"N, 127°54'36"E | Rendzic Leptosol | Medium tall lowland forest |
| Jira | – | 92 | 0°36'19"N, 127°55'08"E | - | Medium tall lowland forest |
| Location 2A | – | 83 | 0°28'42"N, 127°56'9"E | Chromic Hypereutric Cambisol (Hypermagnesic) | Short graminoid scrub |
| Location 2B | – | 82 | 0°28'40"N, 127°56'10"E | Leptic Hypereutric Cambisol (Hypermagnesic) | Short graminoid scrub |
| Location 2C | – | 62 | 0°28'55"N, 127°55'57"E | Hypereutric Vertic Leptic Cambisol (Hypermagnesic) | Short graminoid scrub |
| Sake River | – | 109 | 0°29'18"N, 127°58'57"E | Ferralic Rhodic Hypereutric Cambisol | Medium tall lowland forest |
| Sake South | – | 28 | 0°28'51"N, 127°59'22"E | Ferralic Rhodic Eutric Cambisol (Magnesic) | Medium tall lowland forest |

| | | | | | |
|---|---|---|---|---|---|
| Sake West | – | 105 | 0°29'9"N, 127°57'50"E | Rhodic Plinthic Ferralsol (Eutric, Magnesic) | Medium tall lowland forest |
| Serpentine River | – | 122 | 0°36'19"N, 127°56'50"E | - | Riparian vegetation |
| Uni-Uni | plot 1 | 233 | 0°29'31"N, 127°56'11"E | Geric Plinthic Rhodic Ferralsol | Short graminoid scrub |
| | plot 2 | 160 | 0°29'3"N, 127°56'25"E | Rhodic Hypereutric Cambisol (Magnesic) | Short graminoid scrub |
| Woi Mioseng | – | 45 | 0°30'41"N, 127°54'27"E | Rhodic Hypereutric Cambisol (Magnesic) | Medium tall lowland forest |

**Table 1**. Sites properties showing plot enumeration, location, soil class and dominant vegetation type.

| | Primary minerals | | | | | | | Clay minerals | | | | Iron oxides, Spinels and Al hydroxides | | | |
|---|---|---|---|---|---|---|---|---|---|---|---|---|---|---|---|
| **Location** | **Tremolite** | **Diopside** | **Enstatite** | **Fayalite** | **Palygorskite** | **Calcite** | **Quartz** | **Smectite group clays** | **Chlorite (clinochlore)** | **Talc** | **Serpentine** | **Goethite** | **Hematite** | **Magnetite** | **Gibbsite** |
| Blue Hill | | + | (+) | | | | + | +++ | (+) | | +++ | + | (+) | + | |
| Bukit Limber Plot 1 | | | | | | | + | | | + | ++ (clinochrys.) | +++ | + | + | |
| Bukit Limber Plot 2 | | | | | | | | | | ++ | | +++ | (+) | + | + |
| Casuarina Plot 1 | | + | + | | | | ++ | ++ | | | ++ | + | ++ | ++ | |
| Casuarina Plot 2 | +++ | | | | | | + | ++ | + | (+) | + | + | + | | |
| Casuarina Plot 3 | | | | | | | ++ | | | | | +++ | + | ++ | |
| Doromesmesan Limestone Plot 1 | | | | | | +++ | (+) | | | | | | | | |
| Location 2A | | | | | | | + | +++ | (+) | | + | + | + | (+) | |
| Location 2B | | ++ | + | | + | | | +++ | + | + | | | | | |
| Location 2C | | | | | (+) | | | +++ | | | | | | | |
| Sake River | | | | | | | | (+) | | | (+) | +++ | + | + | |
| Sake South | | | | | | | | (+) | | | + | +++ | ++ | + | |
| Sake West | | | | | | | + | | | (+) | | +++ | | + | |
| Uni-Uni plot 1 | | | | | | | | | | | (+) | +++ | | + | |
| Uni-Uni plot 2 | | | | | | | | ++ | | | +++ | + | ++ | | |
| Woi Mioseng | + | + | | | | | + | + | (+) | | +++ | + | + | + | |

**Table 2.** Mineralogy of the soils (Mineral horizons – 10–25 cm layer) sampled at each site. For the soil in Doromesmesan, the mineralogy was based on the organo-mineral Horizon (0-5 cm layer). +++ (most abundant mineral); ++ (abundant mineral); + (frequent mineral); (+) (detectable traces).

| Location | Al ($g\ kg^{-1}$) | Ca ($g\ kg^{-1}$) | Fe ($g\ kg^{-1}$) | K ($mg\ kg^{-1}$) | Mg ($g\ kg^{-1}$) | Mn ($g\ kg^{-1}$) | Na ($mg\ kg^{-1}$) | Ni ($g\ kg^{-1}$) | P ($mg\ kg^{-1}$) | S ($mg\ kg^{-1}$) | Zn ($mg\ kg^{-1}$) |
|---|---|---|---|---|---|---|---|---|---|---|---|
| Blue Hill | 6.2 | 2.5 | 83 | < LOD | 133 | 0.8 | 26 | 3.5 | 32 | 76 | 69 |
| Bukit Limber plot 1 | 45 | 0.1 | 317 | < LOD | 29 | 1.8 | < LOD | 4.4 | 71 | 299 | 190 |
| Bukit Limber plot 2 | 33 | < LOD | 227 | 51 | 0.9 | 0.2 | 29 | 1.5 | 104 | 582 | 93 |
| Casuarina plot 1 | 7.1 | 5.6 | 67 | 217 | 29 | 0.9 | 155 | 2.1 | 157 | 504 | 70 |
| Casuarina plot 2 | 21 | 14 | 44 | 183 | 26 | 1.0 | 209 | 0.6 | 117 | 368 | 36 |
| Casuarina plot 3 | 22 | 0.6 | 398 | 51 | 2.1 | 6.1 | 24 | 6.4 | 129 | 462 | 285 |
| Doromesmesan Limestone Plot 1 | 26 | 188 | 27 | 145 | 5.2 | 0.5 | 69 | 0.3 | 328 | 635 | 27 |
| Location 2A | 6.4 | 4.2 | 96 | 83 | 20 | 2.4 | 61 | 2.3 | 133 | 474 | 71 |
| Location 2C | 13 | 10.6 | 82 | 483 | 86 | 1.3 | 690 | 1.5 | 92 | 105 | 85 |
| Sake River | 20 | 1.6 | 309 | 61 | 5.3 | 9.5 | 43 | 9.8 | 132 | 467 | 314 |
| Sake South | 10 | 0.2 | 301 | 66 | 14 | 7.1 | 30 | 14 | 295 | 419 | 268 |
| Sake West | 32 | 0.3 | 318 | 30 | 7.0 | 8.1 | < LOD | 8.2 | 111 | 800 | 255 |
| Uni-Uni plot 1 | 39 | 0.1 | 358 | 30 | 0.8 | 2.8 | < LOD | 5.5 | 90 | 748 | 206 |
| Uni-Uni plot 2 | 7.0 | 4.1 | 156 | 100 | 60 | 4.1 | 36 | 4.6 | 48 | 212 | 119 |
| Woi Mioseng | 7.8 | 4.3 | 67 | 114 | 112 | 1.0 | 110 | 2.0 | 135 | 285 | 59 |

< LOD: under the limit of detection

**Table 3**. Total elements for mineral soil (10–25 cm layer) samples from each site.

| Location | Al ($g\ kg^{-1}$) | Ca ($g\ kg^{-1}$) | Fe ($g\ kg^{-1}$) | K ($mg\ kg^{-1}$) | Mg ($g\ kg^{-1}$) | Mn ($g\ kg^{-1}$) | Na ($mg\ kg^{-1}$) | Ni ($g\ kg^{-1}$) | P ($mg\ kg^{-1}$) | S ($mg\ kg^{-1}$) | Zn ($mg\ kg^{-1}$) |
|---|---|---|---|---|---|---|---|---|---|---|---|
| Blue Hill | 6.6 | 7.9 | 67 | 254 | 113 | 1.0 | 83 | 3.4 | 170 | 400 | 89 |
| Bukit Limber plot 1 | 39 | 0.2 | 296 | 56 | 35 | 1.8 | < LOD | 4.5 | 169 | 470 | 186 |
| Bukit Limber plot 2 | 18 | 0.6 | 111 | 324 | 1.9 | 0.2 | 113 | 0.8 | 316 | 1 198 | 57 |
| Casuarina plot 1 | 5.2 | 8.2 | 49 | 311 | 26 | 0.6 | 111 | 1.7 | 262 | 927 | 62 |
| Casuarina plot 2 | 18 | 14 | 40 | 235 | 23 | 0.9 | 180 | 0.6 | 159 | 523 | 36 |
| Casuarina plot 3 | 14 | 5.5 | 272 | 234 | 2.6 | 5.2 | 64 | 5.1 | 194 | 894 | 230 |
| Doromesmesan Limestone Plot 1 | 12 | 190 | 15 | 209 | 4.2 | 0.3 | 85 | 0.2 | 414 | 1 008 | 21 |
| Location 2A | 5.6 | 5.7 | 89 | 117 | 17 | 2.3 | 67 | 2.1 | 164 | 587 | 71 |
| Location 2B | 100 | 24 | 29 | 70 | 15 | 0.5 | 5 797 | 0.1 | < LOD | < LOD | 26 |
| Location 2C | 21 | 21 | 84 | 809 | 65 | 1.4 | 992 | 1.2 | 128 | 80 | 94 |
| Sake River | 17 | 3.4 | 266 | 132 | 4.9 | 8.5 | 69 | 8.4 | 159 | 625 | 277 |
| Sake South | 8.3 | 0.7 | 265 | 114 | 12 | 6.3 | 30 | 12 | 340 | 527 | 237 |
| Sake West | 32 | 1.9 | 313 | 76 | 6.9 | 9.7 | 21 | 7.8 | 178 | 352 | 262 |
| Uni-Uni plot 1 | 40 | 2.8 | 341 | 66 | 1.1 | 4.6 | 21 | 5.7 | 155 | 615 | 222 |
| Uni-Uni plot 2 | 8.1 | 5.2 | 180 | 141 | 39 | 4.1 | 46 | 4.9 | 74 | 200 | 132 |
| Woi Mioseng | 7.8 | 5.2 | 57 | 251 | 87 | 0.9 | 115 | 1.8 | 223 | 547 | 62 |

< LOD: under the limit of detection

**Table 4.** Total elements for organo-mineral soil (0–5 cm layer) samples from each site.

| Location | Co (mg kg$^{-1}$) | Fe (mg kg$^{-1}$) | Mg (mg kg$^{-1}$) | Mn (mg kg$^{-1}$) | Ni (mg kg$^{-1}$) | Zn (mg kg$^{-1}$) |
|---|---|---|---|---|---|---|
| Blue Hill | 0.2 | 46 | 1 409 | 4.0 | 75 | 0.7 |
| Bukit Limber plot 1 | 0.3 | 19 | 216 | 3.0 | 14 | 0.3 |
| Bukit Limber plot 2 | 0.1 | 369 | 4.9 | 2.3 | 4.5 | 0.5 |
| Casuarina plot 1 | 1.5 | 182 | 1 068 | 20 | 335 | 3.8 |
| Casuarina plot 2 | 1.4 | 141 | 1 032 | 47 | 110 | 2.0 |
| Casuarina plot 3 | 27 | 59 | 95 | 180 | 119 | 2.8 |
| Doromesmesan Limestone Plot 1 | 0.1 | 13 | 69 | 6.0 | 2.4 | 0.5 |
| Location 2A | 0.6 | 82 | 911 | 15 | 158 | 1.6 |
| Location 2C | 0.2 | 28 | 688 | 7.4 | 25 | 0.5 |
| Sake River | 12 | 37 | 176 | 146 | 208 | 3.4 |
| Sake South | 4.0 | 11 | 552 | 4.5 | 704 | 4.1 |
| Sake West | 16 | 30 | 63 | 50 | 17 | 0.4 |
| Uni-Uni plot 1 | 3.2 | 71 | 2.2 | 122 | 4.0 | 0.4 |
| Uni-Uni plot 2 | 1.3 | 70 | 1 353 | 20 | 267 | 1.9 |
| Woi Mioseng | 0.7 | 61 | 965 | 13 | 107 | 1.0 |

**Table 5.** DTPA-extractable elements for mineral soil (10–25 cm layer) samples from each site.

| Location | Co (mg kg$^{-1}$) | Fe (mg kg$^{-1}$) | Mg (mg kg$^{-1}$) | Mn (mg kg$^{-1}$) | Ni (mg kg$^{-1}$) | Zn (mg kg$^{-1}$) |
|---|---|---|---|---|---|---|
| Blue Hill | 0.5 | 31 | 1 032 | 10 | 140 | 2.4 |
| Bukit Limber plot 1 | 0.7 | 18 | 352 | 7.2 | 24 | 0.6 |
| Bukit Limber plot 2 | 0.1 | 1 065 | 145 | 6.9 | 11 | 1.3 |
| Casuarina plot 1 | 2.7 | 147 | 1 176 | 33 | 375 | 9.4 |
| Casuarina plot 2 | 0.6 | 80 | 949 | 19 | 156 | 3.2 |
| Casuarina plot 3 | 15 | 42 | 209 | 55 | 518 | 11 |
| Doromesmesan Limestone Plot 1 | 0.6 | 20 | 196 | 35 | 6.0 | 2.2 |
| Location 2A | 0.9 | 120 | 784 | 21 | 243 | 3.1 |
| Location 2B | 0.1 | 5.7 | 593 | 7.4 | 0.1 | 0.2 |
| Location 2C | 0.3 | 20 | 701 | 9.3 | 15 | 0.7 |
| Sake River | 11 | 38 | 164 | 146 | 276 | 5.1 |
| Sake South | 4.7 | 15 | 529 | 5.4 | 773 | 5.1 |
| Sake West | 5.5 | 26 | 53 | 94 | 8.7 | 0.8 |
| Uni-Uni plot 1 | 2.2 | 38 | 13 | 145 | 12 | 1.1 |
| Uni-Uni plot 2 | 1.4 | 59 | 1 275 | 23 | 326 | 2.3 |
| Woi Mioseng | 1.4 | 127 | 1 016 | 24 | 167 | 2.6 |

**Table 6.** DTPA-extractable elements for organo-mineral soil (0–5 cm layer) samples from each site.

| Location | pH | CEC (cmol+ $kg^{-1}$) | K (cmol+ $kg^{-1}$) | Ca (cmol+ $kg^{-1}$) | Mg (cmol+ $kg^{-1}$) | Mn (cmol+ $kg^{-1}$) | Na (cmol+ $kg^{-1}$) | Ni (cmol+ $kg^{-1}$) | %N | %C | %Corg |
|---|---|---|---|---|---|---|---|---|---|---|---|
| Blue Hill | 7.30 | 33 | 0.09 | 12 | 50 | 0.01 | 0.07 | 0.12 | 0.09 | 1.5 | 1.6 |
| Bukit Limber plot 1 | 7.17 | 4.4 | 0.01 | 0.12 | 3.5 | 0.00 | 0.01 | 0.00 | 0.08 | 1.7 | 1.5 |
| Bukit Limber plot 2 | 5.31 | 2.1 | 0.08 | 0.03 | 0.13 | 0.01 | 0.04 | 0.01 | 0.36 | 6.0 | 5.3 |
| Casuarina plot 1 | 6.49 | 41 | 0.40 | 6.1 | 31 | 0.03 | 0.08 | 0.12 | 0.56 | 8.2 | 8.1 |
| Casuarina plot 2 | 6.23 | 23 | 0.21 | 5.7 | 25 | 0.14 | 0.09 | 0.06 | 0.37 | 5.9 | 6.7 |
| Casuarina plot 3 | 5.61 | 29 | 0.09 | 1.4 | 2.0 | 0.17 | 0.04 | 0.23 | 0.38 | 4.9 | 5.8 |
| Doromesmesan Limestone Plot 1 | 8.16 | 54 | 0.19 | 53 | 1.9 | < LOD | 0.12 | < LOD | 0.56 | 13 | 7.6 |
| Location 2A | 6.86 | 38 | 0.17 | 13 | 21 | 0.02 | 0.08 | 0.10 | 0.55 | 7.3 | 6.9 |
| Location 2C | 7.00 | 32 | 0.09 | 18 | 12 | 0.00 | 0.06 | 0.00 | 0.11 | 2.0 | 1.9 |
| Sake River | 6.11 | 13 | 0.11 | 5.8 | 4.2 | 0.14 | 0.11 | 0.29 | 0.46 | 5.6 | 5.2 |
| Sake South | 5.92 | 17 | 0.15 | 0.28 | 13 | 0.29 | 0.08 | 1.4 | 0.48 | 5.3 | 4.8 |
| Sake West | 4.76 | 5.1 | 0.03 | 1.1 | 1.2 | 0.30 | 0.02 | 0.15 | 0.18 | 1.9 | 1.8 |
| Uni-Uni plot 1 | 4.07 | 2.0 | 0.05 | 0.17 | 0.07 | 0.24 | 0.01 | 0.01 | 0.36 | 4.5 | 4.2 |
| Uni-Uni plot 2 | 6.91 | 39 | 0.16 | 3.5 | 33 | 0.06 | 0.06 | 0.27 | 0.29 | 3.8 | 3.8 |
| Woi Mioseng | 6.06 | 21 | 0.08 | 0.28 | 19 | 0.00 | 0.04 | 0.03 | 0.36 | 4.6 | 5.0 |

< LOD: under the limit of detection

**Table 7.** pH, exchangeable cations ($cmol^{+}$ $kg^{-1}$) and nitrogen and carbon content for mineral soil (10–25 cm layer) samples from each site. Abbreviations: Cation Exchange Capacity (CEC), % of soil total nitrogen (%N), % of soil total carbon (%C), % of soil organic carbon (%Corg).

| Location | pH | CEC (cmol+ $kg^{-1}$) | K (cmol+ $kg^{-1}$) | Ca (cmol+ $kg^{-1}$) | Mg (cmol+ $kg^{-1}$) | Mn (cmol+ $kg^{-1}$) | Na (cmol+ $kg^{-1}$) | Ni (cmol+ $kg^{-1}$) | %N | %C | %Corg |
|---|---|---|---|---|---|---|---|---|---|---|---|
| Blue Hill | 7.10 | 39 | 0.18 | 18 | 22 | 0.01 | 0.06 | 0.01 | 0.43 | 7.9 | 5.2 |
| Bukit Limber plot 1 | 6.96 | 7.5 | 0.05 | 0.37 | 6.5 | < LOD | 0.01 | < LOD | 0.23 | 3.0 | 2.6 |
| Bukit Limber plot 2 | 4.65 | 5.2 | 1.2 | 1.8 | 4.1 | 0.21 | 0.57 | 0.06 | 1.7 | 35 | 33 |
| Casuarina plot 1 | 6.34 | 61 | 0.76 | 15 | 40 | 0.05 | 0.14 | 0.08 | 1.0 | 23 | 16 |
| Casuarina plot 2 | 6.78 | 45 | 0.42 | 12 | 27 | 0.06 | 0.09 | 0.05 | 0.53 | 9.4 | 9.3 |
| Casuarina plot 3 | 5.98 | 28 | 0.52 | 20 | 5.9 | 0.42 | 0.20 | 0.39 | 0.98 | 17 | 17 |
| Doromesmesan Limestone Plot 1 | 7.41 | 64 | 0.35 | 62 | 4.6 | 0.01 | 0.21 | < LOD | 0.98 | 22 | 16 |
| Location 2A | 6.74 | 24 | 0.20 | 20 | 13 | 0.01 | 0.09 | 0.03 | 0.60 | 9.9 | 8.8 |
| Location 2B | 6.90 | 28 | 0.01 | 18 | 9.8 | 0.01 | 0.35 | < LOD | 0.01 | 0.42 | 0.41 |
| Location 2C | 8.07 | 45 | 0.20 | 35 | 14 | 0.01 | 0.06 | < LOD | 0.08 | 2.0 | 1.5 |
| Sake River | 6.49 | 17 | 0.26 | 9.9 | 4.4 | 017 | 0.21 | 0.26 | 0.68 | 11 | 9.5 |
| Sake South | 6.01 | 20 | 0.26 | 2.0 | 14 | 0.18 | 0.08 | 1.2 | 0.60 | 7.6 | 6.9 |
| Sake West | 6.59 | 8.7 | 0.07 | 6.0 | 1.4 | < LOD | 0.02 | < LOD | 0.21 | 2.7 | 2.5 |
| Uni-Uni plot 1 | 5.77 | 4.3 | 0.03 | 2.9 | 0.38 | 0.21 | 0.01 | 0.01 | 0.38 | 6.5 | 5.8 |
| Uni-Uni plot 2 | 6.66 | 21 | 0.17 | 5.0 | 31 | 0.06 | 0.04 | 0.24 | 0.31 | 4.2 | 4.0 |
| Woi Mioseng | 6.86 | 37 | 0.24 | 3.7 | 31 | 0.03 | 0.09 | 0.04 | 0.63 | 11 | 10 |

< LOD: under the limit of detection

**Table 8.** pH, exchangeable cations ($cmol^{+}\ kg^{-1}$) and nitrogen and carbon content for organo-mineral soil (0–5 cm layer) samples from each site. Abbreviations: Cation Exchange Capacity (CEC), % of soil total nitrogen (%N), % of soil total carbon (%C), % of soil organic carbon (%Corg).

| Sites | Leaves | | Mineral soils | | | Organic soils | | |
|---|---|---|---|---|---|---|---|---|
| | **Hyperaccumulators** | **Non-hyperaccumulators** | **Ni-DTPA** (mg $kg^{-1}$) | **Ni-CEC** ($cmol^{+}$ $kg^{-1}$) | **Ni-T** (g $kg^{-1}$) | **Ni-DTPA** (mg $kg^{-1}$) | **Ni-CEC** ($cmol^{+}$ $kg^{-1}$) | **Ni-T** (g $kg^{-1}$) |
| Blue Hill | n.d | 375 (< LOD–2824) | 75 | 0.012 | 3.5 | 140 | 0.001 | 3.4 |
| Bukit Limber plot 1 | 851 | 255 (< LOD–21439) | 14 | < LOD | 4.4 | 24 | < LOD | 4.5 |
| Bukit Limber plot 2 | n.d | 8.7 (< LOD–95) | 4.5 | 0.001 | 1.5 | 11 | 0.006 | 0.8 |
| Casuarina plot 1 | 11819 (1808–18636) | 454 (< LOD–15904) | 335 | 0.012 | 2.1 | 375 | 0.008 | 1.7 |
| Casuarina plot 2 | 10946 (10728–11163) | 357 (< LOD–13762) | 110 | 0.006 | 0.6 | 156 | 0.005 | 0.6 |
| Casuarina plot 3 | 6395 (1473–11317) | 293 (< LOD–2473) | 119 | 0.023 | 6.4 | 518 | 0.039 | 5.1 |
| Doromesmesan Limestone Plot 1 | 8.1 | n.d | 2.4 | < LOD | 0.3 | 6.0 | < LOD | 0.2 |
| Location 2A | 15817 | 14 (< LOD–45) | 158 | 0.010 | 2.3 | 243 | 0.003 | 2.1 |
| Location 2C | 152 | 4.1 (< LOD–32) | 25 | < LOD | 1.5 | 15 | < LOD | 1.2 |
| Sake River | 1821 (215–5179) | 351 (< LOD–3344) | 208 | 0.029 | 9.8 | 276 | 0.026 | 8.4 |
| Sake South | 3721 (25–22178) | 955 (< LOD–15934) | 704 | 0.144 | 14 | 773 | 0.119 | 12 |
| Sake West | 815 (147–1203) | 36 (< LOD–182) | 17 | 0.015 | 8.2 | 8.7 | < LOD | 7.8 |
| Uni-Uni plot 1 | 6871 (986–11141) | 587 (< LOD–7191) | 4.0 | 0.001 | 5.5 | 12 | 0.001 | 5.7 |
| Uni-Uni plot 2 | 3917 (2825–5014) | 409 (< LOD–12814) | 267 | 0.027 | 4.6 | 326 | 0.024 | 4.9 |
| Woi Mioseng | 6030 (1117–10943) | 2.8 (< LOD–17) | 107 | 0.003 | 2.0 | 167 | 0.004 | 1.8 |

< LOD: under the limit of detection

n.d.: no data

**Table 9.** Ni distribution in leaf samples (mg $kg^{-1}$) and soil samples for each site. Abbreviations: Extractable Ni (Ni-DTPA, mg $kg^{-1}$), Exchangeable Ni (Ni-CEC, cmol+ $kg^{-1}$) and Ni total (Ni-T, g $kg^{-1}$), no data (n.d).

| Site | Family | Species | Al mg kg$^{-1}$ |
|---|---|---|---|
| Uni-Uni Plot 2 | – | – | 14 500 |
| Bukit Limber Plot 1 | – | – | 1 630 |
| Bukit Limber Plot 1 | – | – | 3 260 |
| Bukit Limber Plot 2 | Cunoniaceae | *Schizomeria serrata* | 4 160 |
| Bukit Limber Plot 2 | Rubiaceae | *Psychotria* sp. | 1 510 |
| Bukit Limber Plot 2 | Theaceae | *Gordonia* sp. | 5 120 |
| Bukit Limber Plot 2 | Lauraceae | *Cryptocarya* sp. | 36 300 |
| Bukit Limber Plot 2 | Symplocaceae | *Symplocos lucida* | 12 100 |
| Bukit Limber Plot 2 | Melastomataceae | *Melastoma* sp. | 6 740 |
| Bukit Limber Plot 2 | Myrtaceae | *Syzygium* sp. | 12 800 |
| Bukit Limber Plot 2 | Rubiaceae | *Psychotria* sp. | 18 300 |
| Bukit Limber Plot 2 | Symplocaceae | *Symplocos maliliensis* | 46 300 |
| Bukit Limber Plot 2 | Symplocaceae | *Symplocos henschelii* | 31 200 |
| Jira Plot 1 | – | – | 35 000 |
| Jira Plot 1 | – | – | 17 800 |

**Table 10.** Aluminium (mg kg$^{-1}$) hyperaccumulator plant records (identified and unidentified specimens) from the Weda Bay area.

| Species | Plant part | Ca mg kg$^{-1}$ | K mg kg$^{-1}$ | Mg mg kg$^{-1}$ | Mn mg kg$^{-1}$ | P mg kg$^{-1}$ | S mg kg$^{-1}$ | Zn mg kg$^{-1}$ | Co mg kg$^{-1}$ | Ni mg kg$^{-1}$ |
|---|---|---|---|---|---|---|---|---|---|---|
| *Amyema cuernosensis* | leaves | 9495 | 3648 | 10 559 | 56 | 361 | 761 | 18 | 4.0 | 262 |
| | | 8211 | 4619 | 9525 | 53 | 382 | 706 | 16 | 3.9 | 242 |
| | | 10 978 | 2732 | 11 654 | 68 | 341 | 899 | 24 | 6.1 | 314 |
| | | 7202 | 7102 | 8737 | 48 | 536 | 823 | 13 | 3.4 | 231 |
| | flowers | 1205 | 18 897 | 3419 | 28 | 1801 | 870 | < LOD | < LOD | 42 |
| | haustoria | 4803 | 2866 | 1324 | 7 | 186 | 738 | 22 | < LOD | 8.6 |
| | twigs | 5966 | 2740 | 3843 | 15 | 486 | 518 | 16 | 0.04 | 0.6 |
| | wood | 4653 | 2089 | 1130 | 129 | 217 | 253 | 19 | 16 | 170 |
| *Ficus trachypison* | roots | 11 459 | 2365 | 4742 | 264 | 173 | 380 | 24 | 60 | 621 |
| | leaves | 12 356 | 1576 | 14 593 | 74 | 418 | 1200 | 21 | < LOD | 194 |
| | | 15 838 | 1272 | 18 176 | 100 | 330 | 1114 | 29 | 3.8 | 228 |
| | | 12 716 | 2046 | 15 873 | 82 | 477 | 1126 | 17 | 4.0 | 228 |
| | twigs | 7524 | 2136 | 4016 | 16 | 385 | 813 | 18 | 0.1 | 2.8 |
| | wood | 6698 | 669 | 1454 | 10 | 105 | 255 | 5.1 | 0.02 | 0.5 |

< LOD: under the limit of detection

**Table 11.** Elemental concentrations (mg kg$^{-1}$) in the mistletoe *Amyema cuernosensis* (Loranthaceae) and the host *Ficus trachypison* (Moraceae).